

Slot Jamming Effect and Mitigation Between LTE-LAA and WLAN Systems With Heterogenous Slot Durations

Yao Ma, *Senior Member, IEEE*, Daniel G. Kuester, *Senior Member, IEEE*, Jason Coder, and William Young
Member, IEEE

Abstract—To improve spectrum sharing between long-term evolution (LTE) license assisted access (LAA) and incumbent systems such as wireless local area networks (WLANs) in unlicensed spectrum, listen before talk (LBT) has been proposed as a candidate for LAA channel access. To allow for a robust spectrum sensing performance, LBT may use a backoff-slot duration that is substantially larger than its WLAN counterpart. There is potential for an unknown backoff slot-jamming (SJ) effect, which may significantly decrease channel access probability (CAP) and throughput of LAA-LBT links. In this paper, we study the SJ effect and propose an effective anti-SJ (ASJ) LBT scheme. To gain theoretical insight, we develop a new performance analysis approach on coexisting systems with different slot durations. We model the LAA backoff process with super-counters, provide an in-depth analysis of the backoff process, and derive key performance indicator (KPI) statistics. These KPIs include backoff hold time, successful transmission probability, CAP, and throughput. Simulation results thoroughly validate our analytical results, and show that the ASJ-LBT scheme is effective in mitigating the SJ effect. These results fill a major technical gap in spectrum sharing research and may be extended to support system optimization and coexistence analysis of other heterogeneous systems.

Index Terms—CSMA/CA; LTE-LAA; MAC-layer Performance Analysis; Wireless Spectrum Sharing; WLAN.

I. INTRODUCTION

A. Background and Motivations

Congestion and scarcity of available spectrum resources motivate research on unlicensed spectrum sharing between long-term evolution license assisted access (LTE-LAA) and the incumbent systems, such as Institute of Electrical and Electronics Engineers (IEEE) 802.11 wireless local area network (WLAN) [1]–[8]. The 3rd Generation Partnership Project (3GPP) has considered the use of listen before talk (LBT) as a possible candidate to enable constructive coexistence between LAA and incumbent systems [4], [5]. Besides 3GPP, the European Telecommunications Standards Institute (ETSI) has defined unlicensed spectrum sharing procedures via LBT

[7], [8]. Various aspects of LTE-LAA and WLAN coexistence have been extensively studied, including experimental and field test results [4]–[6], performance analysis [16]–[20], and optimization methods (e.g., [11]–[13]). WLAN uses carrier sense multiple access with collision avoidance (CSMA/CA) in the medium access control (MAC) layer, whereas load-based LBT may use a similar CSMA/CA protocol but with different specifications.

The WLAN idle slot duration is $9 \mu\text{s}$ for several popular physical-layer specifications in the 5 GHz industrial, scientific, and medical (ISM) band [10]. Regarding LAA and WLAN coexistence, their backoff idle slot durations can be either identical or different. In the first setup, the LAA idle slot duration is assumed to be equal to its WLAN counterpart. This is convenient for system design and analysis, but may not provide adequate time for channel sensing. Typically, a limited portion in an idle slot duration is used for channel sensing, such as the clear channel assessment (CCA) duration in WLAN. When the slot duration is $9 \mu\text{s}$, the actual time for sensing is as low as $4 \mu\text{s}$ for LAA and WLAN systems [9], [10]. Each LAA node requires adequate channel sensing durations for the robust and reliable detection of channel activity. This is even more important when sensing occurs on multipath fading channels when a low signal to noise ratio (SNR) may be experienced.

In the second setup, the LAA slot duration can be larger than its WLAN counterpart. Since an LAA small cell typically has a larger coverage area than a WLAN contention zone and also experiences more mutual interference, there is a practical need to consider an LAA slot duration larger than $9 \mu\text{s}$ to achieve a more reliable channel sensing performance. In 3GPP technical reports [4], [5], the LAA backoff idle slot duration can be up to $20 \mu\text{s}$. In the ETSI standards [7], [8] pertaining to unlicensed spectrum sharing in a few 5 GHz frequency bands, the LBT idle slot duration is set to $18 \mu\text{s}$ in [7] and at least $9 \mu\text{s}$ in [8]. Though the second setup is technically useful, there are two problems: First, heterogeneous slot durations may cause a slot jamming (SJ) effect; second, the performance evaluation is challenging due to the lack of prior art on modelling and analysis of this setup. The SJ effect has been originally described in our preliminary result [19]. The SJ causes WLAN links to have channel access advantage and significantly decreases channel access probability (CAP) and throughput of LAA-LBT links. A straightforward mitigation of SJ is to significantly reduce the contention window (CW) size

Manuscript received June 8, 2018; revised December 6, 2018 and February 4, 2019; accepted February 5, 2019. The editor coordinating the review of this paper and approving it for publication was Prof. Zaher Dawy.

U.S. Government work not protected by U.S. copyright.

This paper was presented in part at the IEEE International Conference on Communications (ICC), May 2017.

Yao Ma, Daniel G. Kuester, and Jason Coder are with Communications Technology Laboratory, National Institute of Standards and Technology, 325 Broadway, Boulder, Colorado, USA.

William Young participated in this work when he was affiliated with NIST, USA. He is now with the MITRE Corporation.

of LAA links. However, this may cause substantially increased chance of collisions, and still may not be effective. To treat the root-cause of the SJ problem, we develop a new LBT scheme that uses variable slot duration to effectively mitigate it.

In general, the backoff-slot durations can be non-identical in different CSMA/CA-based systems, such as IEEE 802.15, IEEE 802.11, and LTE-LAA LBT systems. Hence, analyzing the case of heterogeneous backoff-slot durations will have important theoretical and practical value, which is useful for future coexistence applications of heterogeneous systems.

In this paper, we address the challenging problem of design and performance analysis of LAA-LBT-based coexistence systems with heterogeneous slot durations. The contributions are highlighted as follows:

- We show that with heterogeneous backoff-slot durations between LAA and WLAN systems, there is a previously-unknown backoff-slot jamming effect to LAA nodes based on an original LBT.¹ We propose an anti-SJ (ASJ)-LBT scheme to mitigate this negative effect.
- For both the original-LBT and the proposed ASJ-LBT schemes, we develop a novel analytical tool to model the non-identical backoff-slots with super-counters and weighted probability transition paths. Then, we provide a thorough performance analysis on key performance indicators (KPIs), such as the backoff counter hold time, successful transmission probability (STP), CAP, and throughput of both LAA and WLAN systems.
- We program the related LBT algorithms and implement extensive Monte Carlo simulations, which validate the accuracy of all of the analytical results. Select throughput result is also validated by our software defined radio (SDR) experimental test, which is designed and reported in [21]. Numerical results show that while the SJ effect is detrimental, the proposed ASJ-LBT scheme can significantly alleviate the SJ effect in terms of throughput and STP.

The new techniques developed in this paper fill a major gap in coexistence design and analysis of LAA-LBT-based spectrum sharing systems, and can be extended to the analysis of other CSMA/CA based heterogeneous wireless systems. The technical insight and method provided by this work may be used for KPI optimization of coexisting systems, and to support flexible slot duration design in future 3GPP and ETSI unlicensed spectrum access standards.

B. Related Work

The impact of heterogeneous slot durations in coexisting LAA-LBT and WLAN systems has not been adequately studied. Available methods face formidable challenges to address the case of non-equal idle backoff-slot durations. A popular approach for CSMA/CA performance analysis for a WLAN system is developed in [14], [15], and has been extended in [16]–[18], [20] to coexistence analysis of LAA and WLAN systems. However, extending this framework to model complex system interactions appears intractable when

these systems have non-identical slot durations. For example, this method does not provide a clear procedure to model and compute the backoff wait time per counter reduction (CR). Furthermore, it is not clear how to incorporate the backoff time information (even when available) in this method to analyze the throughput.

Recently, a more powerful method on CSMA/CA performance analysis is provided in [22]–[24], in which explicit models of the backoff hold time and non-traditional statistics are developed to compute the MAC layer throughput. However, the methods in [22]–[24] consider only a WLAN system, and assume identical backoff idle slot durations among all links. How to extend this approach to the performance evaluation of multiple coexistence systems with heterogeneous slot durations is not clear.

Regarding joint optimization LTE-LAA and WLAN systems, several schemes have been proposed in [11]–[13] and addressed various system and fairness constraints. Yet, the effect of non-identical backoff slot durations is not modelled or analyzed therein.

Coexistence analysis between IEEE 802.11 WLAN and IEEE 802.15.4 systems has recently been implemented in [25], where the 802.15.4 devices are assumed to have a backoff-slot duration three times as large as their counterpart WLAN nodes. This method, however, cannot be used for the LAA-LBT and WLAN coexistence analysis. Besides differences in the MAC protocols between LTE-LAA and IEEE 802.15.4, a 802.15.4 device does not have the backoff-slot frozen requirement as the LAA node. Thus, we need to develop a new analytical technique to solve the problem at hand.

From the review of the above, there is a significant technical gap on the modelling and analysis of slot-heterogeneous CSMA/CA systems, especially the case that LAA backoff-slot duration is larger than the WLAN counterpart. In our preliminary result [19], an ASJ-LBT scheme is proposed and analyzed, but the SJ effect of the original LBT scheme is not modelled or analyzed. In this paper, we perform a thorough performance analysis of both original-LBT and ASJ-LBT schemes, and make extensive comparisons. The obtained analytical and simulation results can provide a guideline for performance optimization of coexistence slot-heterogeneous systems.

The remainder of this paper is organized as follows: Section II presents an LBT-based LAA and WLAN coexistence system model, describes the SJ effect, and presents a new ASJ-LBT scheme. Section III defines a preliminary mathematical model for coexistence analysis. Section IV presents a coexistence performance analysis for LTE-LAA with original-LBT using a novel super-counter model assuming heterogeneous slot durations. Section V presents the analysis of ASJ-LBT scheme based on a more complicated super-counter model. Section VI validates all the analytical results via Monte Carlo simulations, as well as an SDR test result, and compares the performance of original and ASJ LBT schemes. Conclusions are provided in Section VII. For ease of reference, some symbols, expressions and their definitions are listed in Table I.

¹Here, the original-LBT refers to the LBT schemes given in [4], [5] with slight revisions, as shown in Fig. 1.

TABLE I: Definition of select symbols and expressions frequently used in this paper.

Symbol or Expression	Definition
$T_{L,0}$ (or $T_{W,0}$)	Time per counter reduction (CR) in an LAA (or WLAN) link.
$T_{S,L}$ (or $T_{F,L}$)	Time of successful (or failed) transmission in an LAA link.
τ_L^{LO} (or τ_L^{GO})	Locally (or globally) observed channel access probability (CAP) of an LAA link.
$\hat{P}_{i,L}$ (or $P_{i,L}$)	Observed LAA channel idle probability by an LAA (or WLAN) link.
$\hat{P}_{S,L}$ (or $P_{S,L}$)	Observed LAA successful transmission probability (STP) by an LAA (or WLAN) link.
$\pi_{S,L}$ (or $\pi_{S,W}$)	State probability of successful transmission of an LAA (or WLAN) link.
$\pi_{R,L,k}$ (or $\pi_{F,L,k}$)	State probability of backoff (or failed transmission) at stage k of an LAA link.

II. SYSTEM MODEL

Here, we consider a scenario that several LTE-LAA links and WLAN links use CSMA/CA schemes (such as LBT) to coexist in unlicensed bands. The processing flow of an LAA Category 4 LBT scheme is shown in Fig. 1, as adopted from [4], [5] with modifications. In comparison with [4], [5], we switched the order of the blocks “ $z > 0$ ” and “extended CCA”. This revision lets a transmitter that finishes one transmission to wait for an additional idle slot before it restarts the backoff process. This change makes sure that after a channel busy period, the active transmitter that finishes its transmission opportunity (TXOP) does not have priority over the other stations in the next channel access competition. It is consistent with the non-contiguous transmission requirement set by 3GPP and ETSI [4], [7]–[9].

A channel busy duration for basic access scheme is formed by payload duration, T_{SIFS} , T_{ACK} , and T_{DIFS} , where T_{SIFS} , T_{ACK} , and T_{DIFS} refer to short interframe space (SIFS), acknowledgement signal duration, and distributed coordination function (DCF) interframe space (DIFS), respectively. When an LAA transmission is over, the receiver waits for a duration of SIFS, and sends back an ACK signal via the reverse link. Then, after a T_{Defer} silent duration, all links resume backoff countdown.

To facilitate smooth coexistence, we make the following assumptions:

- 1) The LAA extended defer period (T_{Defer}) is set equal to the WLAN DIFS duration (T_{DIFS}).
- 2) Both LAA-LBT and WLAN systems use a similar CSMA/CA protocol with multistage backoff, but with differences on some parameters, such as CW size, maximum backoff stage, slot duration, and payload duration. The LBT and DCF protocols we consider here follow closely those described in [4], [5], [14], [15], [22].
- 3) Failed transmissions are caused by either collisions or low channel SNR. We define packet error rate (PER) to model the effect of low SNR on the KPIs. This is more general than the assumption in [14], [15], [22], [24] that failed transmissions are only caused by collisions.

When $N_s = 1$, in an idle slot of $9 \mu s$, there is an overhead of about $5 \mu s$ which is caused by MAC and physical layer delays, and transmit and receive turn around time, etc. There is about $4 \mu s$ dedicated for CCA sensing [9], [10]. When $N_s = 2$ or 3 , the LAA node has $9 \times 2 - 5 = 13 \mu s$ or $9 \times 3 - 5 = 22 \mu s$ for CCA sensing, respectively. The sensing time ratio between

$N_s = 2$ or 3 vs. $N_s = 1$ is $13/4$ or $22/4$, and this brings about 5.12 dB or 7.4 dB improvement of SNR for channel detection, respectively. Therefore, the non-equal idle slot setup for the LAA is very useful for a low SNR scenario.

A. Slot-Jamming Effect in LAA-LBT with Heterogeneous Slot Durations

We define δ_L and δ_W as the backoff idle slot durations for LAA and WLAN, respectively. In the original-LBT, the idle slot duration δ_L is fixed at $\delta_L = N_s \delta_W$, where N_s is a positive integer.

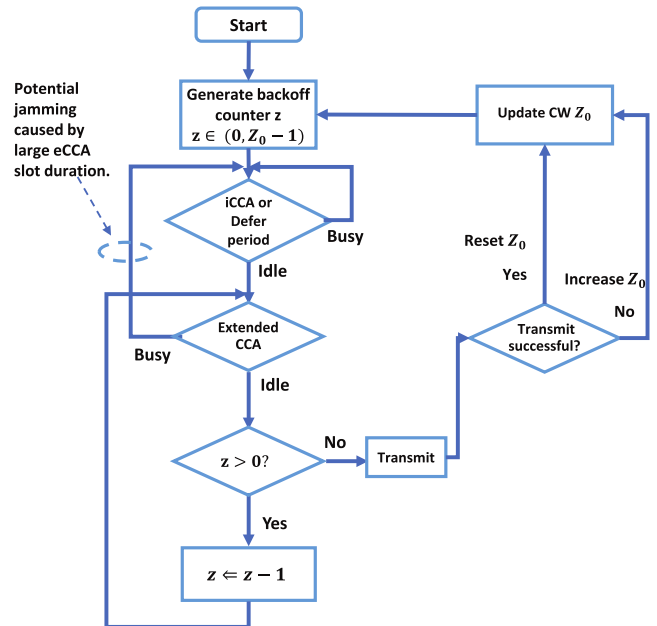


Fig. 1: Flow diagram of LTE downlink LAA LBT Category-4 procedure (aka, an original LBT), adopted from [4], [5] with minor revisions. We mark the backoff SJ effect assuming that the LTE-LAA system has a backoff-slot duration larger than that of the WLAN system.

We point out that when $N_s > 1$, the original-LBT scheme can cause a backoff SJ effect which is disadvantageous to the LAA links. This is not investigated in the available literature (except briefly by our preliminary result in [19]). This SJ effect is illustrated for the original-LBT in Fig. 2 which assumes $N_s = 3$. In the example shown in Fig. 2, an LAA CR takes a longer slot duration ($N_s \delta_W$) than its WLAN counterpart (δ_W),

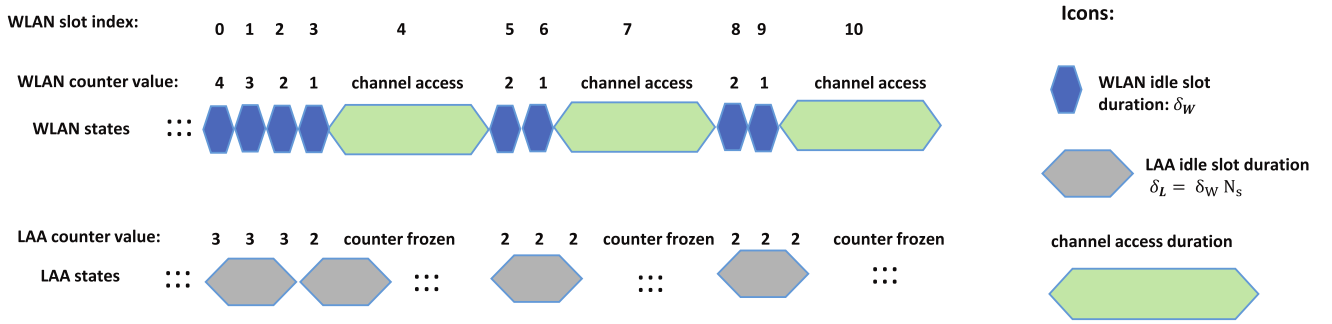


Fig. 2: Backoff counter reduction and transmission process of one LAA link (with original-LBT) and one WLAN link, when the LAA has backoff-slot duration three times as large as that of the WLAN system ($N_s = 3$).

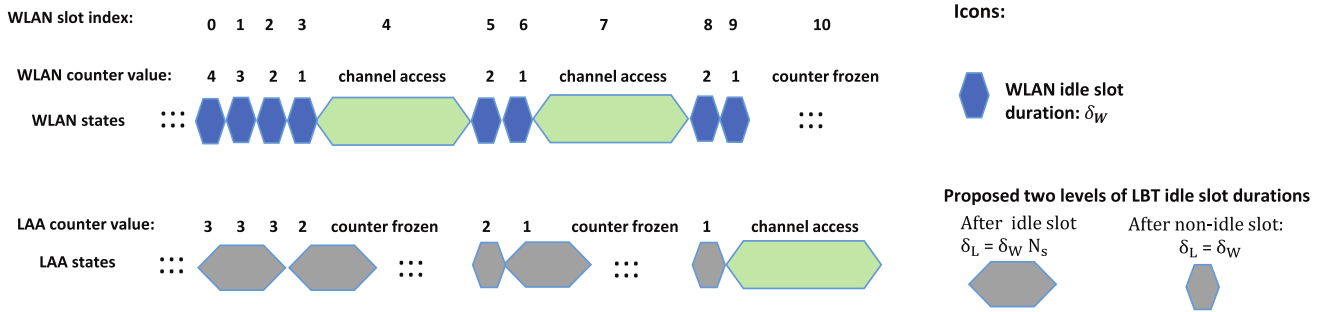


Fig. 3: Backoff counter reduction and transmission process of one LAA link (with the proposed ASJ-LBT) and one WLAN link, when $N_s = 3$.

and before it reaches a slot boundary, a WLAN counter may first reduce to zero and begin a transmission. After the channel busy state is over, the LAA node has to reset the counter value to the state before the WLAN transmission occurs: that is, the reduction can be jammed if there are frequent WLAN transmissions (when $N_s > 1$). The SJ effect happens in WLAN slots 3-9 in Fig. 2, where the LAA counter value remains at two, and its reduction is interfered and jammed by WLAN transmissions. When there are an increased number of WLAN links, the SJ effect will be more severe. Besides the case of LAA and WLAN coexistence with different slot durations, the SJ effect can also happen when two or more LAA systems coexist and have different slot durations.

B. A Countermeasure Scheme: ASJ-LBT

In the LAA backoff CR scheme, shown in Fig. 1 and Fig. 2, an LAA CR occurs in either of the following two cases:

- 1) when the channel becomes idle for $T_{\text{DIFS}} + \delta_L$ right after a channel-busy state;
- 2) the channel becomes idle for δ_L again right after a previous CR.

The SJ effect reduces the CAP and throughput of LAA nodes when $N_s > 1$. To mitigate this problem, we propose an improved LAA CR scheme, where δ_L can be a variable depending on cases 1 and 2 of channel status, and name it the ASJ-LBT scheme. Suppose that an LAA node has maximum backoff stage K (aka. cutoff stage), with CW size Z_k at stage k , for $k = 0, 1, \dots, K$.

The ASJ-LBT Scheme

- 1) Initialize to backoff stage 0 ($k = 0$). Draw counter value $Z \in (1, Z_0)$, where Z_0 is the LAA initial CW size.
- 2) Decrease counter Z by 1 in either of the following cases; otherwise, freeze the counter.
 - case 1: Following a channel busy state, if the channel becomes idle for $T_{\text{DIFS}} + \delta_W$;
 - case 2: After the previous CR, channel is idle again for $\delta_L = N_s \delta_W$.
- 3) If Z is reduced to zero, starts a transmission.
- 4) If the transmission is successful, go to step 1);
- 5) If the transmission fails: if $k < K$, add backoff stage k by 1, draw counter value $Z \in (1, Z_k)$, and go to step 2); and if $k = K$, drop the packet and go to Step 1).

In our proposed ASJ-LBT scheme, in step 2) when any node just finishes a transmission, the channel will be idle for at least $T_{\text{DIFS}} + \delta_W$ duration. This gives an opportunity for all the nodes to reduce their counters by one. In case 1, each LAA node has a slot duration $\delta_L = \delta_W$, so that LAA and WLAN nodes have equal priority in reducing their counter values. After an LAA CR, if the idle period continues (the status becomes case 2), then we still set $\delta_L = N_s \delta_W$, which enables an adequate slot period for channel sensing.

The state transition with CR for the proposed scheme is given in Fig. 3. In WLAN slot indexes 5 and 9 of Fig. 3, the ASJ-LBT scheme allows the LAA CR after each channel busy event, and consequently makes an LAA transmission at slot 9. This is in contrast to that shown in Fig. 2 where the original-LBT has a counter value being jammed to two.

The ASJ-LBT scheme has two advantages over the original-LBT: 1) it significantly mitigates the SJ effect, so that it protects CAP and throughput of LAA links; and 2) it causes only a small impact on channel sensing accuracy. Although the total idle duration used for channel detection in case 1 is reduced from $T_{\text{DIFS}} + N_s \delta_W$ to $T_{\text{DIFS}} + \delta_W$, it is still typically larger than $N_s \delta_W$ (the idle slot duration in case 2). The ASJ-LBT is designed to treat the root cause of the SJ effect, and it may be combined with some CSMA/CA parameter optimization schemes [23], [24] to further provide target KPIs, such as proportional fairness or maximization of throughput.

III. PRELIMINARY MODELLING AND ANALYSIS FOR THE LAA-LBT

To analyze the performance of the original-LBT and ASJ-LBT schemes and make comparisons, we provide a new mathematical modeling of coexistence systems in this section. The results will be used to further analyze both original and ASJ-LBT schemes. The basic formulas for throughput evaluation developed here are fundamentally different from those used in [16]–[18]. Our method has a slight similarity to those given in [22]–[24], but has several major differences and enhancements in modelling and analytical techniques to compute STP, CAP, and transmission backoff duration.

A. A New Mathematical Modeling of Coexistence System

The backoff-and-transmission state transition model for a Category-4 LBT is described in Fig. 4.(a). At stage k ($k = 0, \dots, K$), R_k and F_k are the backoff state and failed transmission state, respectively, and $P_{t,L}$ is the conditional probability of a successful LAA transmission (conditioned on that an LAA transmission starts). The state of a successful transmission is denoted by S . When the transmission in stage K fails, the counter moves to stage 0.

Some detail about one backoff stage (stage k) with $N_s > 1$ is described in Fig. 4.(b), where one LBT idle slot duration is N_s times as large as a WLAN idle slot duration ($N_s > 1$). This significantly changes the interactions between LAA-LBT and WLAN systems in terms of CAP, STP, and throughput, compared to the case of $N_s = 1$. Available analytical approaches are not flexible enough to analyze coexistence performance in this scenario.

Based on the LAA-LBT Markov model of Fig. 4, some CSMA/CA parameters related to LTE and WLAN coexistence are defined here. In this paper, we use subscripts L, W, p, i, S, F to denote LAA, WLAN, payload, idle slot, successful transmission, and failed transmission, respectively.

We define $T_{P,L}$ (and $T_{P,W}$) as payload duration, $T_{S,L}$ (and $T_{S,W}$) as channel access duration caused by a successful transmission (which includes payload, T_{SIFS} , ACK and T_{Defer}), $T_{F,L}$ (and $T_{F,W}$) as channel access duration caused by a failed transmission, and $T_{R,L}$ (and $T_{R,W}$) as total backoff duration for an LAA (and WLAN) node, respectively. Furthermore, for an LAA (and WLAN) node, we define $\pi_{S,L}$ (and $\pi_{S,W}$) as the probability of a successful transmission, $\pi_{F,L}$ (and $\pi_{F,W}$) as the probability of a failed transmission, and $\pi_{R,L}$ (and $\pi_{R,W}$) as the probability of staying in a backoff stage, respectively.

For the basic access schemes in the LAA-LBT system, we define $T_{S,L} = T_{P,L} + T_{\text{SIFS}} + T_{L,\text{ACK}} + T_{\text{DIFS}} + \delta_L$, and $T_{F,L} = T_{S,L}$, where the purpose of δ_L is to remove the channel access priority of the LAA node which just finishes a successful transmission. For the RTS/CTS-type access in the LAA system, we define

$$T_{S,L} = T_{\text{RTS}} + T_{\text{SIFS}} + T_{\text{CTS}} + T_{\text{SIFS}} + T_{P,L} + T_{\text{SIFS}} + T_{L,\text{ACK}} + T_{\text{DIFS}} + \delta_L, \quad (1)$$

$$T_{F,L} = T_{\text{RTS}} + T_{\text{SIFS}} + T_{L,\text{ACK}} + T_{\text{DIFS}} + \delta_L. \quad (2)$$

The $T_{S,W}$, $T_{F,W}$ for WLAN with RTS/CTS access can be obtained, similar to (1)-(2). The time-efficiency throughputs of an LAA link and a WLAN link are, respectively, given by:

$$S_L = \pi_{S,L} T_{P,L} / T_{\text{ave},L} \quad (3)$$

$$S_W = \pi_{S,W} T_{P,W} / T_{\text{ave},W}, \quad (4)$$

where $T_{\text{ave},L}$ (and $T_{\text{ave},W}$) is the average total duration caused by one successful LAA (and WLAN) transmission. The time-efficiency throughput for (3) and (4) refers to the time proportion of successful payload transmission of that link divided by the total observation duration. The payload throughputs in physical layer (which models the losses caused by backoff wait and failed transmissions) are given by $S_L R_L$ and $S_W R_W$, respectively, where R_L and R_W are the channel bit rate (CBR) of LAA and WLAN links.

The $T_{\text{ave},L}$ involved in (3) can be computed from

$$T_{\text{ave},L} = \pi_{S,L} T_{S,L} + \sum_{k=0}^K [\pi_{R,L,k} T_{R,L,k} + \pi_{F,L,k} T_{F,L,k}], \quad (5)$$

where $\pi_{R,L,k}$ and $T_{R,L,k}$ represent the probability of backoff stage k and the incurred hold time, respectively, and $\pi_{F,L,k}$ is the failed transmission probability at stage k . Define $\pi_{F,L,k}$ and $\pi_{R,L,k}$ as the probabilities for failed transmission and backoff at stage k , respectively. Given that the total probability of Markov chain states is unity, we have $\pi_{S,L} + \sum_{k=0}^K [\pi_{R,L,k} + \pi_{F,L,k}] = 1$. Based on the model of Fig. 4(a), we can solve for the state probabilities as:

$$\pi_{S,L} = P_{t,L} / 2, \quad (6a)$$

$$\pi_{R,L,0} = \frac{0.5 P_{t,L}}{1 - (1 - P_{t,L})^{K+1}}, \quad (6b)$$

$$\pi_{R,L,k} = \pi_{R,L,0} (1 - P_{t,L})^k, \quad (6c)$$

$$\pi_{F,L,k} = \pi_{R,L,0} (1 - P_{t,L})^{k+1}, \quad (6d)$$

for $k = 0, \dots, K$. For a Category-3 LBT (when $K = 0$), we have $\pi_{S,L} = 0.5 P_{t,L}$, $\pi_{F,L} = 0.5 (1 - P_{t,L})$, and $\pi_{R,L} = 0.5$. Using a similar procedure, we can obtain $T_{\text{ave},W}$ as

$$T_{\text{ave},W} = \sum_{m=0}^M [\pi_{R,W,m} T_{R,W,m} + \pi_{F,W,m} T_{F,W,m}] + \pi_{S,W} T_{S,W}, \quad (7)$$

where $\pi_{S,W}$, $\{\pi_{F,W,m}\}_{m=0,\dots,M}$, and $\{\pi_{R,W,m}\}_{m=0,\dots,M}$ can be computed using equations similar to (6a)-(6d), replacing k, K and $P_{t,L}$ by m, M and $P_{t,W}$, respectively. $P_{t,W}$ is

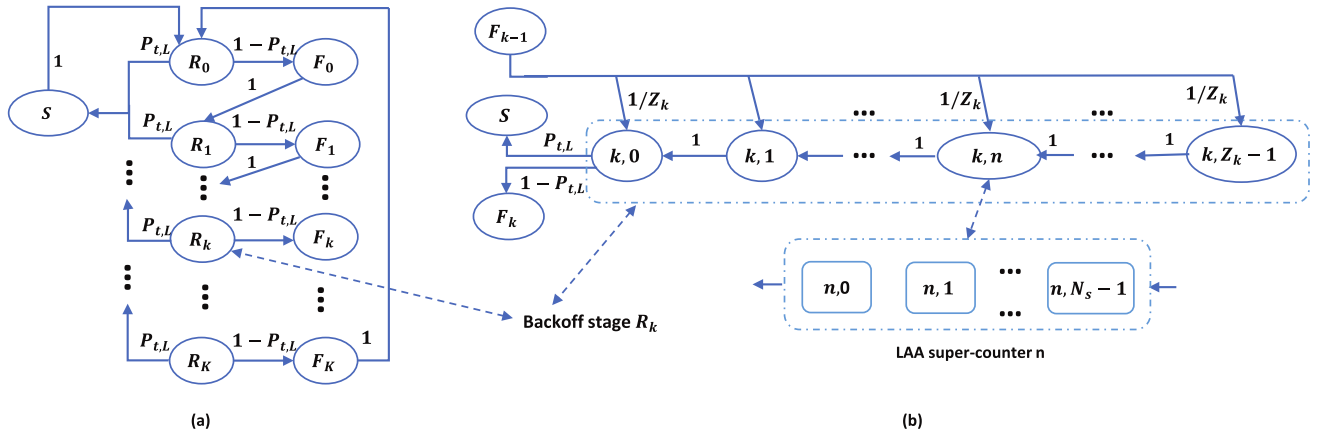


Fig. 4: Markov model for the LTE-LAA category-4 LBT procedure in coexistence with WLAN, when overall state transition has $K + 1$ stages, and backoff stage k (state R_k) is illustrated (with $N_s > 1$).

the conditional STP of a WLAN node given that it starts a transmission.

We define the CAPs of an LAA node and a WLAN node as τ_L and τ_W , respectively, and their expressions are provided by (33) and (34) in Appendix A. We can solve for $P_{t,L}$, $P_{t,W}$, τ_L , and τ_W jointly by expressing $P_{t,L}$ and $P_{t,W}$ as functions of τ_L and τ_W and other parameters.

To compute throughput, we still need to find backoff durations $T_{R,L,k}$ (for LAA) and $T_{R,W,m}$ (for WLAN). Their analytical formulas will be developed in Sections IV and V for the original-LBT and ASJ-LBT schemes, respectively.

B. Equal Slot Duration ($N_s = 1$)

For $N_s = 1$ we develop a new method which explicitly computes backoff time based on enumerating all the probability paths of one CR. This probability path enumeration method is also partially described in our preliminary result [20]. This feature allows us to more conveniently analyze the backoff process for $N_s > 1$. Here, we try to develop an approach that explicitly calculates the durations spent on the backoff stage for both LAA and WLAN nodes. Our method uses multiple feedforward probability paths to compute a CR time. It is different than [22], [23], which use a feedback probability path method.

When $N_s = 1$, it follows that

$$P_{t,L} = (1 - \tau_W)^{n_W} (1 - \tau_L)^{n_L - 1} (1 - P_{PE,L}), \quad (8)$$

$$P_{t,W} = (1 - \tau_W)^{n_W - 1} (1 - \tau_L)^{n_L} (1 - P_{PE,W}), \quad (9)$$

where $P_{PE,L}$ and $P_{PE,W}$ are the transmission PERs due to the low SNR, in the LTE-LAA and WLAN systems, respectively. When the backoff moves to stage k for an LAA node (or m for a WLAN node), the initial counter may take values uniformly from $(1, Z_K)$ and $(1, W_m)$, respectively. We assume that all transmitting and listening nodes have one idle slot, right after the transmission and T_{DIFS} silent duration. So, all nodes may use this idle slot of duration δ_W to reduce counter value by one when $N_s = 1$. Consequently, after finishing a transmission, an LAA (or WLAN) node has equivalently an initial counter value which is uniformly distributed in range $(0, Z_K - 1)$ (or

$(0, W_m - 1)$) at stage k (or m) when $N_s = 1$. It follows that $T_{R,W,m} = \frac{W_m - 1}{2} T_{W,0}$, and

$$T_{R,L,k} = \frac{Z_k - 1}{2} T_{L,0}, \quad (10)$$

where $T_{L,0}$ and $T_{W,0}$ are the hold-time per CR at LAA and WLAN nodes, respectively. Their expressions are derived in Appendix B and are given by (35) and (36), respectively. Our method of computing $T_{L,0}$ and $T_{W,0}$ is accurate and new, and uses only feedforward probability paths when $N_s = 1$. A comparison with a recent method on analyzing $T_{W,0}$ in [22] is given in Appendix C.

Eq. (10) holds for $N_s = 1$, and the ASJ-LBT scheme when $N_s \geq 1$. Note that, however, (10) is slightly different for the original-LBT scheme when $N_s > 1$, which is provided by (16) in Section IV. By applying results in (5)–(10), (35), and (36) into (3) and (4), the throughput of the coexisting LAA and WLAN links with $N_s = 1$ can be readily evaluated. The purpose of showing the case of $N_s = 1$ is to set up a benchmark to compare with available methods, and define some variables that will be used for the case $N_s > 1$ for both the original-LBT and ASJ-LBT schemes.

IV. COEXISTENCE PERFORMANCE ANALYSIS FOR THE ORIGINAL-LBT ($N_s > 1$)

Based on results in Section III, we now proceed to analyze the performance of the original-LBT scheme, assuming $N_s > 1$.

A. Modeling of LAA Backoff Process

To address the complicated interaction between LAA and WLAN nodes in the backoff countdown process, we develop a new approach that is significantly different than those in the available literature [14]–[18], [22], [23], [25].

Refer to super-counter n in Fig. 5, where the stage index k is suppressed for brevity. In Fig. 5, the detail of LAA CR is modeled by assuming $N_s > 1$ and N_s is an integer. At counter value n , the slot duration δ_L is split into N_s sub-counters, each with duration δ_W , and denoted as $(n, 0)$, $(n, 1)$, \dots , $(n, N_s - 1)$

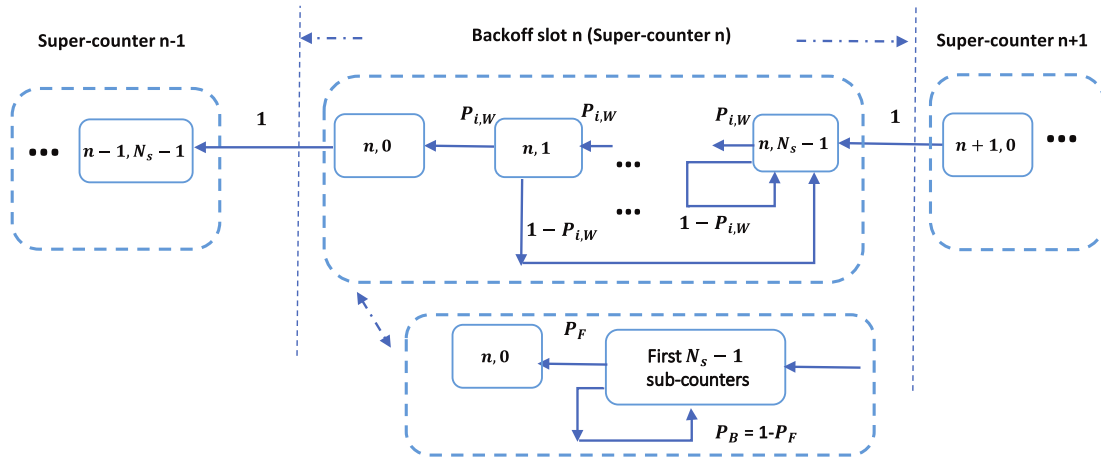


Fig. 5: Proposed super-counter model for the original LTE-LAA LBT procedure in coexistence with WLAN (when $N_s > 1$).

1), respectively. At sub-counter $(n, N_s - 1)$, when no WLAN node transmits (with probability $P_{i,W}$), the process moves to sub-counter $(n, N_s - 2)$; otherwise, when any WLAN node transmits (with probability $1 - P_{i,W}$), the process resets and restarts from sub-counter $(n, N_s - 1)$. This phenomenon holds until sub-counter $(n, 1)$. At sub-counter $(n, 0)$, the LAA counter finishes its CR, and the transition time to next LAA sub-counter $(n - 1, N_s - 1)$ can be computed based on six events illustrated in Fig. 15.

B. Successful Transmission Probabilities

We define $P_W(\text{WCR})$ as the probability that only WLAN counter reduction (WCR) can happen in an idle slot of duration δ_W , and $P_W(\text{JCR})$ as the probability that LTE-LAA and WLAN joint counter reduction (JCR) may happen, respectively, as observed by a WLAN node. Similarly, we define $P_L(\text{WCR})$ and $P_L(\text{JCR})$ as the corresponding probabilities of WCR and JCR, as observed by an LAA node.

We define τ_L^{LO} and τ_L^{GO} as the locally observed (LO) and globally observed (GO) CAPs of an LAA node, respectively. τ_L^{LO} is the LAA CAP when an idle LAA slot of duration δ_L ($= N_s \delta_W$) is observed, and τ_L^{GO} is the LAA CAP based on a δ_W -duration idle slot. When $N_s = 1$, $\tau_L^{\text{LO}} = \tau_L^{\text{GO}} = \tau_L$. But when $N_s > 1$, $\tau_L^{\text{GO}} \leq \tau_L^{\text{LO}}$ due to an SJ effect. Since a WLAN node uses a fixed δ_W -duration idle slot, its CAP τ_W is the same based on either local or global observations.

Define the probabilities of sub-counters $(n, 0), (n, 1), \dots, (n, N_s - 1)$ as $P_0, P_1, \dots, P_{N_s-1}$, respectively. Note that $\sum_{k=0}^{N_s-1} P_k = 1$ holds. At sub-counters $(n, 1) \dots, (n, N_s - 1)$ only a WLAN node can reduce its counter value, and JCR can happen only at sub-counter $(n, 0)$. Therefore, $P_W(\text{JCR}) = P_0$ and $P_W(\text{WCR}) = 1 - P_W(\text{JCR}) = \sum_{k=1}^{N_s-1} P_k$.

Furthermore, since $P_{k-1} = P_k P_{i,W}$, for $k = 1, \dots, N_s - 1$ (a homogeneous Markov chain), we can determine $P_0, P_1, \dots, P_{N_s-1}$ uniquely. After some manipulations, we obtain $P_{N_s-1} = \frac{1 - P_{i,W}}{1 - P_{i,W}^{N_s}}$, and $P_0 = P_{N_s-1} P_{i,W}^{N_s-1}$. Thus,

$$P_W(\text{JCR}) = \frac{(1 - P_{i,W}) P_{i,W}^{N_s-1}}{1 - P_{i,W}^{N_s}}. \quad (11)$$

Note that in Fig. 5 and deriving (11), we assume a homogeneous Markov for sub-counter state transitions. A more accurate model may be obtained by using a non-homogeneous Markov chain, omitted here for brevity.

For $N_s > 1$, the conditional LAA STP $P_{t,L}$ is observed only at a JCR event. So,

$$P_{t,L} = (1 - \tau_L^{\text{LO}})^{n_L-1} (1 - \tau_W)^{n_W} (1 - P_{\text{PE},L}). \quad (12)$$

In comparison, the conditional WLAN STP $P_{t,W}$ is observed at both WCR and JCR events. Thus, we obtain

$$P_{t,W} = (1 - P_{\text{PE},W}) [P_W(\text{WCR})(1 - \tau_W)^{n_W-1} + P_W(\text{JCR})(1 - \tau_W)^{n_W-1} (1 - \tau_L^{\text{LO}})^{n_L}]. \quad (13)$$

At a WCR event, an LAA transmission cannot happen, and hence the term $(1 - \tau_W)^{n_W-1}$ in (13) denotes the channel-busy probability caused by the other $n_W - 1$ WLAN nodes. Based on the JCR and WCR concept, τ_L^{GO} is given by:

$$\tau_L^{\text{GO}} = \tau_L^{\text{LO}} P_L(\text{JCR}).$$

The average STPs for each LAA and WLAN link based on the original-LBT scheme are, respectively, given by:

$$P_{\text{txS},L}^{\text{Org}} = \tau_L^{\text{GO}} P_{t,L}, \quad (14)$$

$$P_{\text{txS},W}^{\text{Org}} = \tau_W P_{t,W}. \quad (15)$$

For $N_s > 1$, the LAA hold time $T_{R,L,k}$ at stage k is related to $T_{L,0}$ by

$$T_{R,L,k} = \frac{Z_k + 1}{2} T_{L,0}, \quad (16)$$

which is different than (10). We explain this as follows: after an LAA transmission and $T_{\text{DIFS}} + \delta_W$ silent period, the LAA node that just finishes a transmission will draw an initial value $Z \in (1, \dots, Z_k)$. Note that when $N_s = 1$, the δ_W idle slot causes the counter to be reduced immediately and so $Z \in (0, 1, \dots, Z_k - 1)$. However, when $N_s > 1$, the LAA node still needs to wait for additional $(N_s - 1)\delta_W$ idle period to finish a CR (refer to Fig. 5). Thus, we obtain its initial counter value $Z \in (1, \dots, Z_k)$ instead of $(0, 1, \dots, Z_k - 1)$. This causes the average value of Z to be $E[Z] = \frac{Z_k + 1}{2}$ instead of $\frac{Z_k - 1}{2}$. In

comparison, $T_{R,W,m} = \frac{W_m-1}{2}T_{W,0}$ holds for $N_s > 1$ as well, since WLAN links are not subject to the SJ effect. Analytical expressions of $T_{L,0}$ and $T_{W,0}$ for $N_s > 1$ are studied next.

C. Backoff Counter Hold Duration and Throughput

Based on an assumption of independent transitions in the first $N_s - 1$ sub-counters in Fig. 5, we list the probability and duration pairs in Table II. The probability for sub-counter (n, j) is the chance that the LAA sensing process goes to the end of (n, j) , but is reset due to a channel-busy event caused by a WLAN transmission.

In Table II, $\bar{T}_{L,WCR}$ is the average sub-counter hold duration (normalized by its probability) when only WCR occurs. This happens when the LAA backoff is in any of the sub-counters $(n, 1), \dots, (n, N_s - 1)$. WLAN transmissions can cause a feedback path with probability $(1 - P_{i,W})$. Thus,

$$\bar{T}_{L,WCR} = \frac{1}{(1 - P_{i,W})} [P_{S,W}T_{S,W} + P_{F,W}T_{F,W}]. \quad (17)$$

The $\bar{T}_{L,JCR}$ is the average sub-counter hold duration for LAA in $(n, 0)$, for a JCR event, and its expression is the same as (35).

The first to $(N_s - 1)$ th terms in Table II correspond to all the feedback paths with a total probability P_B . When $\bar{T}_{L,WCR} \gg \delta_W$, we can group all feedback paths with an overall probability P_B , and average feedback duration of T_B . The last term $(n, 0)$ in Table II corresponds to the direct feedforward path (without any feedback) with probability P_F and duration T_F . We have:

$$T_F = \bar{T}_{L,JCR} + (N_s - 1)\delta_W, \quad (18)$$

$$T_B \simeq \bar{T}_{L,WCR} + (N_s/2 - 1)\delta_W. \quad (19)$$

We derive the per CR hold durations for LAA and WLAN nodes in Appendix D, and the results are provided by (41) and (42), respectively. By substituting results given by (5)–(7), (12)–(16), (41), and (42) into (3) and (4), the throughput performance of LAA and WLAN systems with the original-LBT and $N_s > 1$ can be computed analytically.

TABLE II: Probability and duration pairs to compute LAA counter hold time of the original-LBT.

Index	Probability	Duration
$(n, N_s - 1)$	$1 - P_{i,W}$	$\bar{T}_{L,WCR}$
$(n, N_s - 2)$	$P_{i,W}(1 - P_{i,W})$	$\delta_W + \bar{T}_{L,WCR}$
\dots	\dots	\dots
$(n, 1)$	$P_{i,W}^{N_s-2}(1 - P_{i,W})$	$(N_s - 2)\delta_W + \bar{T}_{L,WCR}$
$(n, 0)$	$P_{i,W}^{N_s-1}$	$(N_s - 1)\delta_W + \bar{T}_{L,JCR}$

V. COEXISTENCE PERFORMANCE ANALYSIS FOR THE PROPOSED ANTI-SJ LBT ($N_s > 1$)

The analysis of the proposed ASJ-LBT scheme is more challenging than the original-LBT (Assume $N_s > 1$). The ASJ-LBT involves two cases of CRs:

- 1) C1: Channel is idle for $T_{DIFS} + \delta_W$ following a transmission (channel busy); and

- 2) C2: Channel is idle for $\delta_L = N_s\delta_W$ right after a previous CR.

We model the transition paths between the two cases during an LAA CR in Fig. 6. An LAA counter is decomposed into N_s sub-counters, and the paths of current CR depend on the status of the previous CR. Thus, we model cases 1 and 2 explicitly in Fig. 6, and list all the involved probability-duration pairs in Table III.

We explain each path next. Define the probabilities of cases 1 and 2 in Fig. 6 as $\Pr(C_1)$ and $\Pr(C_2)$. It follows that

$$\Pr(C_1) = \Pr(C_1)(1 - \hat{P}_{i,L}P_{i,W}) + [\Pr(C_1) + \Pr(C_2)] \cdot \hat{P}_{i,L}P_{i,W}[1 - \hat{P}_{i,L}P_{i,W}^{N_s}], \quad (20)$$

$$\Pr(C_2) = [\Pr(C_1) + \Pr(C_2)]\hat{P}_{i,L}P_{i,W}P_{i,W}^{N_s-1}. \quad (21)$$

We can verify that equations (20) and (21) are equivalent, as expected. To determine $\Pr(C_1)$ and $\Pr(C_2)$, we need one more equality. The sum probability of all sub-counter states within one CR in Fig. 6 is equal to unity. Thus,

$$\Pr(C_1) + [\Pr(C_1) + \Pr(C_2)]\hat{P}_{i,L}P_{i,W} \cdot (1 + P_{i,W} + \dots + P_{i,W}^{N_s-1}) = 1. \quad (22)$$

Based on (21) and (22), we derive:

$$\begin{aligned} \Pr(C_2) &= \left(\frac{1 - \hat{P}_{i,L}P_{i,W}^{N_s}}{\hat{P}_{i,L}P_{i,W}^{N_s}} + \frac{1 - P_{i,W}^{N_s}}{P_{i,W}^{N_s-1} - P_{i,W}^{N_s}} \right)^{-1} \\ &= \frac{\hat{P}_{i,L}P_{i,W}^{N_s}(1 - P_{i,W})}{1 - P_{i,W} - \hat{P}_{i,L}P_{i,W}^{N_s} + \hat{P}_{i,L}P_{i,W}}, \\ \Pr(C_1) &= \Pr(C_2) \frac{1 - \hat{P}_{i,L}P_{i,W}^{N_s}}{\hat{P}_{i,L}P_{i,W}^{N_s}}. \end{aligned}$$

When $N_s = 1$, (20) and (21) reduce to

$$\Pr(C_1|N_s = 1) = (1 - \hat{P}_{i,L}P_{i,W}),$$

$$\Pr(C_2|N_s = 1) = \hat{P}_{i,L}P_{i,W},$$

as expected. This means that when $N_s = 1$, case 1 corresponds to a channel busy event, which is always followed by DIFS and an idle slot δ_W , and case 2 corresponds to a channel idle event, where all LAA and WLAN nodes stay idle.

A. Successful Transmission Probabilities

We define $\tilde{P}_W(\text{WCR})$ as the probability that only WLAN nodes may reduce counter, and $\tilde{P}_W(\text{JCR})$ as the probability that all LAA and WLAN nodes may reduce counter, respectively, after a δ_W idle slot, observed by the WLAN system. Here, superscript $\tilde{\cdot}$ on P refers to the case of ASJ-LBT. $\tilde{P}_W(\text{WCR})$ is the sum probability the $N_s - 1$ subcells in the right side of the super-counter. When $N_s \geq 2$, we have $\tilde{P}_W(\text{JCR}) = 1 - \tilde{P}_W(\text{WCR})$, and

$$\begin{aligned} \tilde{P}_W(\text{WCR}) &= [\Pr(\tilde{C}_1) + \Pr(\tilde{C}_2)]P_{i,L}\hat{P}_{i,W} \\ &\quad \cdot (1 + \hat{P}_{i,W} + \dots + \hat{P}_{i,W}^{N_s-2}) \\ &= \frac{\hat{P}_{i,W}P_{i,L}(1 - \hat{P}_{i,W}^{N_s-1})}{1 - \hat{P}_{i,W} - P_{i,L}\hat{P}_{i,W}^{N_s} + P_{i,L}\hat{P}_{i,W}}, \end{aligned}$$

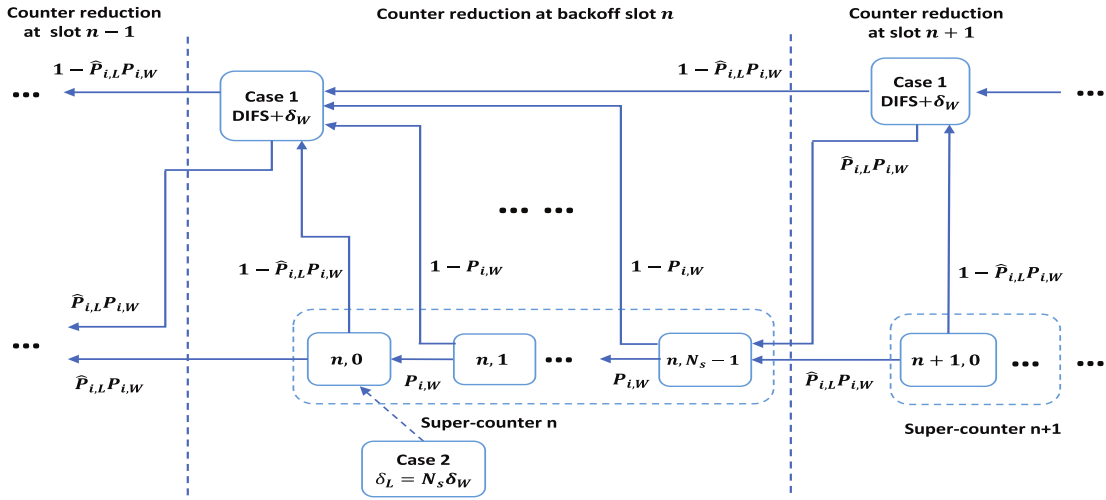


Fig. 6: Proposed backoff model on probability paths for the LAA with ASJ-LBT.

where $\Pr(\tilde{C}_1)$ and $\Pr(\tilde{C}_2)$ are obtained from $\Pr(C_1)$ and $\Pr(C_2)$ by replacing $\hat{P}_{i,L}$ and $P_{i,W}$ with $P_{i,L}$ and $\hat{P}_{i,W}$ therein, respectively. With probability \tilde{P}_W (WCR), all LAA nodes stay silent. Thus, the conditional STP of a WLAN node is given by:

$$P_{t,W} = (1 - P_{PE,W})[\tilde{P}_W(\text{WCR})(1 - \tau_W)^{n_W-1} + \tilde{P}_W(\text{JCR})(1 - \tau_W)^{n_W-1}(1 - \tau_L^{\text{LO}})^{n_L}]. \quad (23)$$

The conditional STP of an LAA node is given by:

$$P_{t,L} = (1 - \tau_L^{\text{LO}})^{n_L-1}(1 - \tau_W)^{n_W}(1 - P_{PE,L}). \quad (24)$$

In (23) and (24), τ_L^{LO} is given by (33). The LAA CAP, based on total number of available idle slots of δ_W durations, is given by:

$$\begin{aligned} \tau_L^{\text{GO}} &= \tau_L^{\text{LO}} P_L(\text{JCR}) \\ &= \tau_L^{\text{LO}} \frac{1 - P_{i,W}}{1 - P_{i,W} - P_{i,W}^{N_s} P_{i,L} + P_{i,W} P_{i,L}}. \end{aligned} \quad (25)$$

The average STPs of each LAA link and WLAN link based on the ASJ-LBT scheme are, respectively, given by:

$$P_{\text{txS},L}^{\text{ASJ}} = P_{t,L} \tau_L^{\text{GO}} = P_{t,L} \tau_L^{\text{LO}} P_L(\text{JCR}), \quad (26)$$

$$P_{\text{txS},W}^{\text{ASJ}} = P_{t,W} \tau_W. \quad (27)$$

Note that τ_L^{LO} and $P_{t,L}$ are based on LAA local observation of idle slots, and are independent of N_s . But τ_L^{GO} and $P_{\text{txS},L}^{\text{ASJ}}$ (based on global observation) are functions of N_s , and provide a clearer illustration of LAA performance when in coexistence with WLAN.

B. Backoff Counter Hold Time and Throughput

Refer to Fig. 6 again. The average hold time for an LAA node $T_{L,0}$ is obtained by summing the duration of each path from the start states to the end states, weighted by the path probability. The probability and duration pair of each path is listed in Table III.

In Table III, the last three columns list each path, and its corresponding probability and duration. The first row is for the

direct path through the regular counter on the top side, from case 1 to case 1 which is a channel busy event. The 2nd to $(N_s + 1)$ th rows are for the paths through the super-counter on the bottom side starting from either case 1 or 2 and ending in case 1. The $(N_s + 2)$ th term is for reaching sub-counter $(n, 0)$, from case 2 to case 2. As an example, consider sub-counter $(n, N_s - 1)$ which has probability $\Pr(C_1, C_2)(1 - P_{i,W})$ to exit the counter n . The factor $\Pr(C_1, C_2)$ is the probability that the LAA backoff goes to counter value n from a previous counter $n + 1$ (either case 1 or 2), and is given by:

$$\Pr(C_1, C_2) = [\Pr(C_1) + \Pr(C_2)]P_{i,W}\hat{P}_{i,L}. \quad (28)$$

The other factor $(1 - P_{i,W})$ is the probability that at the end of the first τ_W duration in super-counter n , at least one WLAN transmissions start and are detected by this LAA node. After this channel busy event is over, the LAA node moves to case 1, shortens its slot duration to δ_W , reduces the counter value to $n - 1$, and thus it exits this counter. The $\bar{T}_{L,\text{WCR}}$ is the average channel busy time when the WCR occurs (normalized by its probability), given by:

$$\bar{T}_{L,\text{WCR}} = \frac{1}{(1 - P_{i,W})} [P_{S,W} T_{S,W} + P_{F,W} T_{F,W}].$$

In the last row of Table III, when sub-counter $(n, 0)$ is reached, $\bar{T}_{L,\text{JCR}}$ is the average channel busy duration for a CR. $\bar{T}_{L,\text{JCR}}$ is given by (35), where the involved probabilities of $N_s = 1$ are replaced by those for the case of $N_s > 1$. $T_{L,0}$ can be computed by summing up all the probability-weighted durations in Table III, resulting in

$$T_{L,0} \simeq \frac{1}{\Pr(C_1) + \Pr(C_2)} \sum_{n=1}^{N_s+2} P_{n,L} T_{n,L}, \quad (29)$$

where the normalization by factor $\Pr(C_1) + \Pr(C_2)$ is used, because an LAA node transmits only upon the two idle cases with sum probability $\Pr(C_1) + \Pr(C_2)$. The minor approximation in (29) is caused by facts such as that a homogeneous Markov chain in a super-counter CR is modelled. A better

TABLE III: Probability and duration pairs to compute LAA counter hold time of the ASJ-LBT.

Index	Sub-counter index	Probability	Duration
1	$C_1 \rightarrow C_1$	$\Pr(C_1)(1 - \hat{P}_{i,L}P_{i,W})$	$\bar{T}_{L,JCR}$
2	$(n, N_s - 1)$	$\Pr(C_1, C_2)(1 - P_{i,W})$	$\bar{T}_{L,WCR}$
3	$(n, N_s - 2)$	$\Pr(C_1, C_2)(1 - P_{i,W})P_{i,W}$	$\bar{T}_{L,WCR} + \delta_W$
...
N_s	$(n, 1)$	$\Pr(C_1, C_2)(1 - P_{i,W})P_{i,W}^{N_s-2}$	$\bar{T}_{L,WCR} + (N_s - 2)\delta_W$
$N_s + 1$	$(n, 0)$	$\Pr(C_1, C_2)(1 - P_{i,W}\hat{P}_{i,L})P_{i,W}^{N_s-1}$	$\bar{T}_{L,JCR} + (N_s - 1)\delta_W$
$N_s + 2$	$(n, 0)$	$\Pr(C_1, C_2)\hat{P}_{i,L}P_{i,W}^{N_s}$	$N_s\delta_W$

accuracy may be obtained if a non-homogenous model of sub-counter transition is used. The average CR duration can also be expressed as

$$T_{L,0} = \frac{\Pr(C_1)T_{L,0|C_1} + \Pr(C_2)T_{L,0|C_2}}{\Pr(C_1) + \Pr(C_2)}, \quad (30)$$

where $T_{L,0|C_1}$ and $T_{L,0|C_2}$ are the CR durations conditioned on starting states C_1 and C_2 , respectively. Assuming that $\bar{T}_W \gg \delta_W$ and $\bar{T}_{L,JCR} \gg \delta_W$, we have $T_{L,0|C_2} \simeq P_{i,W}\hat{P}_{i,L}[(1 - P_{i,W}^{N_s-1})\bar{T}_{L,WCR} + P_{i,W}^{N_s-1}(1 - \hat{P}_{i,L}P_{i,W})\bar{T}_{L,JCR}]$, and $T_{L,0|C_1} \simeq T_{L,0|C_2} + (1 - P_{i,W}\hat{P}_{i,L})\bar{T}_{L,JCR}$. We obtain an approximate formula for $T_{L,0}$ as

$$T_{L,0} \simeq P_{i,W}\hat{P}_{i,L}[(1 - P_{i,W}^{N_s-1})\bar{T}_{L,WCR} + P_{i,W}^{N_s-1}(1 - \hat{P}_{i,L}P_{i,W})\bar{T}_{L,JCR}] + \frac{\Pr(C_1)(1 - \hat{P}_{i,L}P_{i,W})}{\Pr(C_1) + \Pr(C_2)}\bar{T}_{L,JCR}. \quad (31)$$

By use of the concept of JCR and WCR, $T_{W,0}$ for a WLAN node is derived as

$$T_{W,0} \simeq \tilde{P}_W(\text{WCR})\tilde{T}_{W,WCR} + \tilde{P}_W(\text{JCR})\tilde{T}_{W,JCR}, \quad (32)$$

where

$$\begin{aligned} \tilde{T}_{W,WCR} &= \hat{P}_{S,W}T_{S,W} + \hat{P}_{F,W}T_{F,W} + \hat{P}_{i,W}\delta_W, \\ \tilde{T}_{W,JCR} &= \hat{P}_{i,W}P_{i,L}\delta_W + (\hat{P}_{S,W}T_{S,W} + \hat{P}_{F,W}T_{F,W})P_{i,L} \\ &\quad + (P_{S,L}T_{S,L} + P_{F,L}T_{F,L})\hat{P}_{i,W} \\ &\quad + (1 - \hat{P}_{i,W})(1 - P_{i,L})T_{F,M}. \end{aligned}$$

By substituting results given by (5)–(7), (10), (23), (24), (31), and (32) into (3) and (4), the throughput performance of LAA-LBT and WLAN systems with the ASJ-LBT and $N_s > 1$ can be readily evaluated.

VI. NUMERICAL RESULTS

In this section, we provide both analytical and simulation results of the spectrum sharing performance of LTE-LAA and WLAN links. Both the original-LBT and the proposed ASJ-LBT schemes are simulated, and the results are compared with analytical formulas derived in Sections IV and V. In our Monte-Carlo computer simulation, we define and track three global events at each slot: channel idle, successful transmission, and failed transmission (caused by either collision or low receiver SNR). We also track four local events for every LAA and WLAN link: channel idle, channel busy (counter frozen), successful transmission, and failed transmission. On each

parameter setting, we ran 10^6 mixed time slots to generate the simulation results.

Our simulation method and codes, when simplified to the case of only WLAN links and after minor changes, provide numerical results that fit well to the methods given by [14], [22]. To further validate our simulation method, we provide an SDR test result for two CSMA/CA links with different slot durations. The setup and method of experiment were presented in detail in [21], where we varied the slot duration ratio (N_s) of two coexistence CSMA/CA links, and recorded the throughput for the original LBT and the ASJ-LBT schemes. The throughput was normalized by the physical-layer rate, and the payload duration is 3 ms. The simulation and SDR measured results are provided in Fig. 7, which shows that the ASJ-LBT reduces the SJ effect compared to the original LBT scheme for link 2 which has a larger slot duration. In addition, the simulation result (in lines) matches well with SDR measured result (in markers).

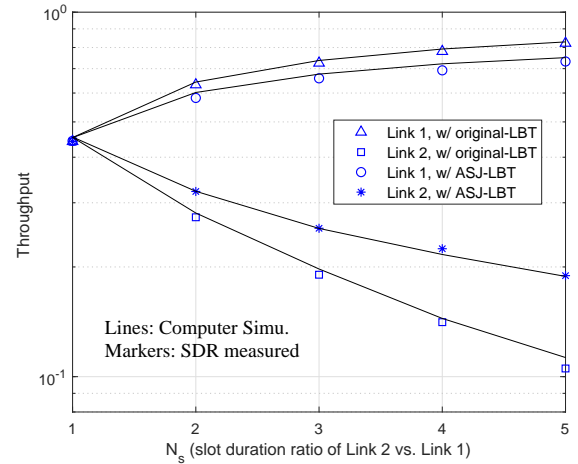
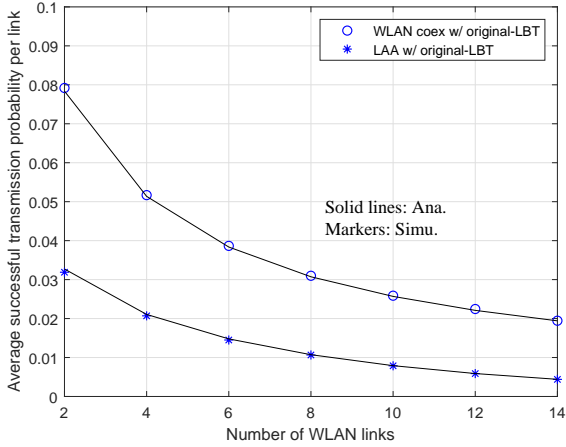
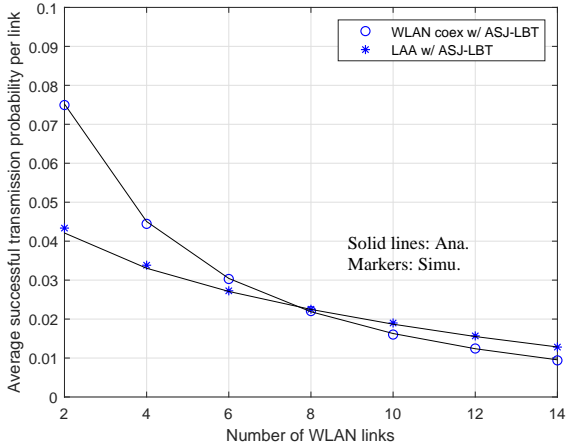


Fig. 7: Throughput of two CSMA/CA links, when $N_s = 1 \sim 5$. $CW = 16$ for both links, without retransmission.

From here on, we consider larger link numbers (n_L and n_W) and compare analytical and simulation results. We set payload durations for LAA and WLAN as $T_{P,L} = 2$ ms and $T_{P,W} = 1$ ms, $Z_0 = W_0 = 16$, and $\delta_W = 9 \mu\text{s}$. The LAA successful transmission and collision channel-busy durations in an RTS/CTS mode are given by (1) and (2), respectively. We assume that the WLAN and LAA systems have channels fully overlapped in the 5 GHz ISM band. Every analytical curve in



(a)



(b)

Fig. 8: Average successful transmission probability per link of the LAA and WLAN systems vs. n_W , when $N_s = 2$, $K = 1$, $M = 3$, $Z_0 = W_0 = 16$, $n_L = n_W$, and with RTS/CTS schemes. (a) Original LBT and (b) ASJ-LBT.

each figure is accompanied by another curve based on Monte Carlo simulation result. Comparison between analytical and simulation results illustrates a very close match.

The average STPs for the original-LBT (see (14)) and the ASJ-LBT (see (26)) are provided in Fig. 8 (a) and (b), respectively, assuming $N_s = 2$, $K = 1$, $M = 3$, $Z_0 = W_0 = 16$, and $n_L = n_W$. Fig. 8 shows that as n_W increases from 2 to 14, the STP of the original-LBT scheme reduces from about 0.032 to 0.005, but the STP of the ASJ-LBT scheme decreases only from about 0.042 to 0.013, which significantly enhances the performance compared to the original-LBT.

Next, the backoff hold durations per CR of LAA and WLAN systems are illustrated in Fig. 9 for the original-LBT and ASJ-LBT schemes assuming $N_s = 3$, $K = 1$, $M = 3$, $Z_0 = W_0 = 16$, and $n_L = n_W$. As n_W increases, the counter hold time of the original-LBT scheme increases almost exponentially, from about 1 ms to about 3.4 ms. In comparison, the hold time of the ASJ-LBT scheme varies from about 0.6 ms to about

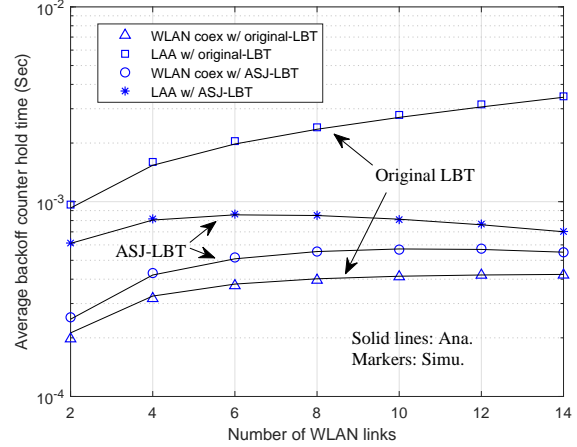


Fig. 9: Backoff counter hold time per reduction of LAA and WLAN systems vs. n_W , when $N_s = 3$, $K = 1$, $M = 3$, $Z_0 = W_0 = 16$, $n_L = n_W$, and with RTS/CTS schemes.

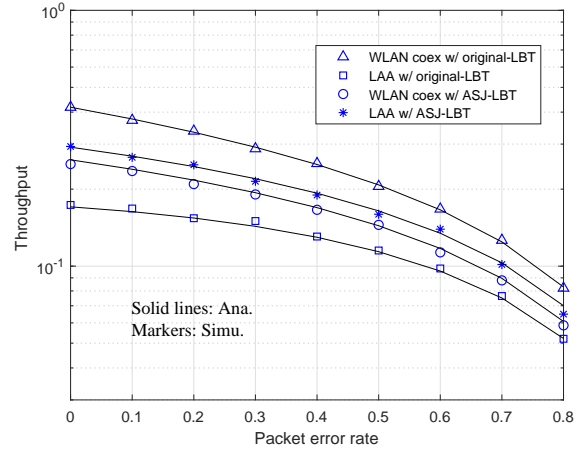


Fig. 10: System throughput of LAA and WLAN vs. PER ($P_{EP,L} = P_{EP,W}$), when $N_s = 2$, $K = M = 3$, $W_0 = Z_0 = 16$, $n_L = n_W = 10$, and with basic access schemes.

0.85 ms and then drops to 0.7 ms, and the gap between the WLAN and LAA hold durations decreases as n_W increases. The backoff time of the ASJ-LBT is significantly less than that of the original-LBT, indicating a better CAP performance.

We show the time-efficiency system throughput of the LTE-LAA and WLAN under the effect of PER in Figs. 10 and 11, assuming the basic access and RTS/CTS schemes, respectively. We assume that the RTS/CTS packet experiences the same PER as the payload packet. Figs. 10 shows that when the PER increases from 0 to 0.8, the throughputs of the LAA and WLAN systems decrease significantly. For example, the throughput of the LAA with original-LBT reduces from about 0.17 to about 0.05. In comparison, when the LAA and WLAN both use RTS/CTS schemes, their throughput decreases with PER, but more gracefully. This is because with the RTS/CTS handshaking, the failed packets cause much smaller time loss than the basic access scheme.

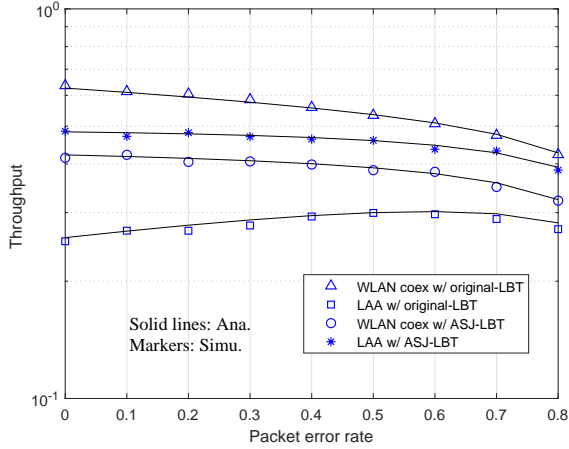


Fig. 11: System throughput of LAA and WLAN systems vs. PER ($P_{EP,L} = P_{EP,W}$), when $N_s = 2$, $K = M = 3$, $W_0 = Z_0 = 16$, $n_L = n_W = 10$, and with RTS/CTS access schemes.

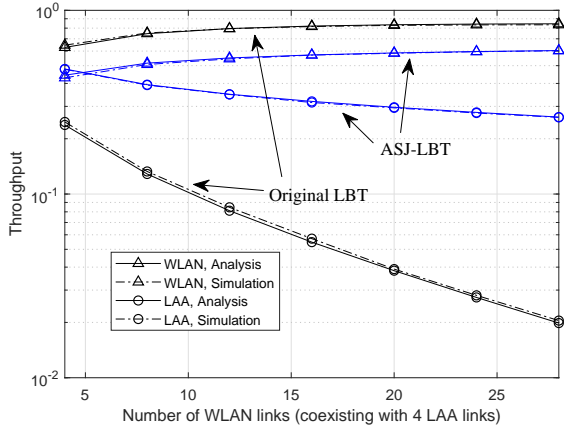
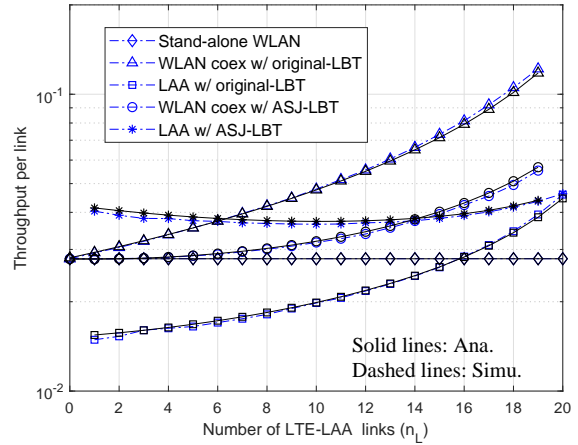


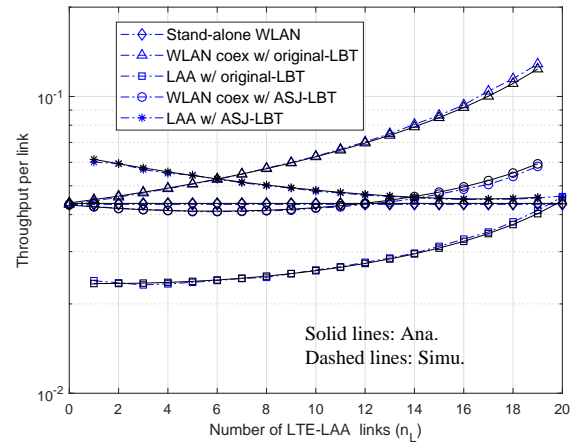
Fig. 12: System throughput of LAA and WLAN vs. n_W , when $N_s = 3$, $K = 1$, $M = 3$, $Z_0 = W_0 = 16$, $n_L = 4$, and with RTS/CTS schemes.

We consider a fixed $n_L = 4$ but an increasing n_W in Fig. 12. As n_W increases from 4 to 28, the system throughput of the LAA system (with the original-LBT) decreases from about 0.24 to about 0.02. In comparison, the LAA throughput (with the ASJ-LBT) decreases from about 0.48 to 0.26 when $N_s = 3$. This greatly mitigates the effect of slot jamming caused by larger LAA slot durations. In summary, the ASJ-LBT avoids the problem of very low throughput which the original-LBT may suffer from due to the SJ, while maintaining a substantially larger sensing slot duration than its WLAN counterpart (when $N_s > 1$).

We study the constructive coexistence between WLAN and LAA systems based on different LBT and access schemes when $n_W + n_L = 20$ and n_L increases from 0 to 20. We consider 2 cases: (1) WLAN uses basic access and LAA uses RTS/CTS access, and (2) both WLAN and LAA systems use RTS/CTS. The throughput per link is given in Fig. 13 (a) and (b) for the two cases, respectively. For comparison purposes,



(a)



(b)

Fig. 13: Throughput per link in the LAA and WLAN systems vs. n_L , when $N_s = 2$, $K = M = 3$, $W_0 = Z_0 = 16$, and $n_W + n_L = 20$. (a) WLAN basic access and LAA RTS/CTS access; (b) Both WLAN and LAA use RTS/CTS.

we also show the performance of a standalone WLAN system ($n_W = 20$ and $n_L = 0$). Fig. 13 shows that the per-link-throughput of standalone WLAN is about 0.028 (case 1) or 0.044 (case 2). As n_L increases, in case 1 with ASJ-LBT the throughput of each LAA link changes within about 0.037 to 0.045, and the throughput of each WLAN link increases from 0.028 to 0.057. These throughputs are comparable to each other, and they are higher than the basic-access WLAN throughput of 0.028. In case 2 with ASJ-LBT the per-link throughputs of coexisting LAA and WLAN systems are close to or better than that of the standalone WLAN system, though the relative advantage is reduced because the standalone WLAN system uses an efficient RTS/CTS scheme.

In comparison, with original-LBT, in case 1 the WLAN throughput per link increases from about 0.028 to 0.12 as n_L increases, but the LAA throughput per link stays below 0.028 unless $n_L \geq 16$. In case 2, the per-link-throughput of LAA with original LBT stays lower than that of a standalone

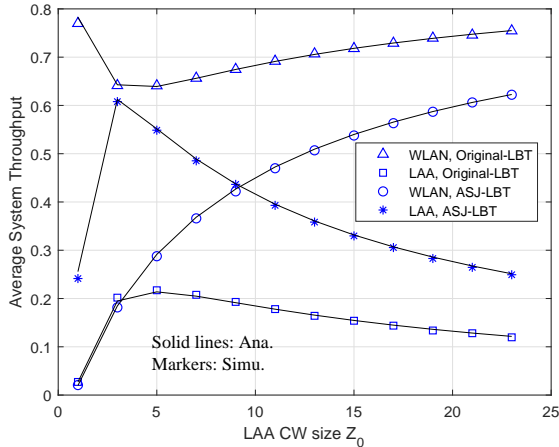


Fig. 14: System throughput of LAA and WLAN vs. Z_0 , when $N_s = 2$, $K = M = 3$, $W_0 = 16$, $n_L = n_W = 10$, and with RTS/CTS access schemes.

WLAN system for $n_L \leq 19$. This shows that the LAA with original-LBT suffers from SJ effect and the coexistence cannot be regarded as constructive. From the result of Fig. 13 we draw observation that the ASJ-LBT and the use of LAA RTS/CTS scheme can effectively support constructive coexistence for the two systems with heterogeneous slot durations.

It is shown in [23], [24] that in a WLAN system with heterogeneous throughput requirements, the target throughput ratio of links may be achieved by adjusting the CSMA/CA parameters, such as the CW size. We show that the ASJ-LBT design can support system optimization in Fig. 14, when $N_s = 2$, $K = M = 3$, $W_0 = 16$, $n_L = n_W = 10$, with RTS/CTS access schemes. As the LAA CW size Z_0 increases, there is a cross-over point in the throughput of the LAA and WLAN systems based on the ASJ-LBT. Thus, we can select proper Z_0 to enable the LAA and WLAN systems to achieve a large range of different throughput ratios (including the case of equal throughput). But with the original LBT, the throughput of the LAA is much lower than that of the WLAN system for all the considered $Z_0 \in (1, 23)$. This indicates that the original LBT cannot effectively support throughput optimization in this case.

VII. CONCLUSION

In this paper, we have studied the impact of heterogeneous backoff-slot durations on the MAC-layer performance of LTE-LAA coexisting with WLAN transmissions. We first pointed out a slot-jamming effect due to differences in backoff idle slot durations among LAA-LBT and WLAN systems, and proposed an anti-SJ LBT scheme to mitigate this problem. We have developed a novel and powerful analytical framework with several new features, such as backoff super-counter, enumerated probability-duration paths, and different probability-time scales captured by WLAN only CR and joint CR events. Then, we provided analytical results on the backoff counter hold time, successful transmission probability, channel access probability (locally and globally observed) and throughput. We

have implemented in-depth programming of LAA-LBT and WLAN schemes and extensive computer simulations, which have verified all of the analysis results. We have also provided an SDR experimental result to validate our simulation method. Numerical results confirm that the original-LBT may suffer from an SJ effect when $N_s > 1$, and our proposed ASJ-LBT scheme is effective in mitigating this problem. This result provides support for a system design when a larger LAA sensing duration than the WLAN counterpart is necessary (e.g., due to low SNR), and will be useful for the related system optimization work. The new analytical tool lays a solid theoretical foundation to evaluate effect of heterogeneous slot scales in unlicensed spectrum sharing systems, and may support related standardization effort in the 3GPP and ETSI.

APPENDIX A

DERIVATION OF CAPS OF LAA AND WLAN NODES

We derive τ_L using a procedure given in our preliminary result [18], where τ_L is the sum of probabilities at backoff counters $(0, 0), (1, 0), \dots, (K, 0)$ shown in Fig. 4. The related state transition probabilities are given by:

$$\begin{aligned} P(0, k|j, 0) &= P_{t,L}/Z_0, \text{ for } j \in [0, K-1], \\ P(0, k|K, 0) &= (1 - P_{t,L})/Z_0, \text{ and} \\ P(j, k|j, k+1) &= 1, \text{ for } j \in [0, K], k \in [0, Z_j - 2]. \end{aligned}$$

We define $P_{j,k}$ as the stationary probability of state (j, k) . It follows that:

$$\begin{aligned} P_{j,0} &= (1 - P_{t,L})^j P_{0,0}, \text{ for } j \in [0, K], \text{ and} \\ P_{j,k} &= \frac{Z_j - k}{Z_j} P_{j,0}, \text{ for } k \in [0, Z_j - 1]; j \in [0, K]. \end{aligned}$$

Since the total probability of all states is 1, i.e., $\sum_{j=0}^K \sum_{k=0}^{Z_j-1} P_{j,k} = 1$, we obtain

$$P_{0,0} = \left[0.5 \sum_{j=0}^K (1 - P_{t,L})^j (1 + Z_j) \right]^{-1}.$$

The CAP of an LAA node is given by:

$$\begin{aligned} \tau_L &= \sum_{j=0}^K P_{j,0} = P_{0,0} \frac{1 - (1 - P_{t,L})^{K+1}}{P_{t,L}} \\ &= \frac{2[1 - (1 - P_{t,L})^{K+1}]}{P_{t,L} \sum_{j=0}^K (1 - P_{t,L})^j (1 + Z_j)}. \end{aligned} \quad (33)$$

The CAP for an LAA Category-3 node (when $K = 0$) is derived as

$$\tau_L = 2/(1 + Z_0).$$

Using a similar procedure to the above, τ_W is derived as:

$$\tau_W = \frac{2(1 - (1 - P_{t,W})^{M+1})}{P_{t,W} \sum_{m=0}^M (1 - P_{t,W})^m (1 + W_m)}. \quad (34)$$

APPENDIX B

DERIVATION OF CR DURATIONS $T_{L,0}$ AND $T_{W,0}$ WHEN

$$N_s = 1$$

Let \hat{P} and P denote probabilities observed by a node when observing its own system (e.g., state of LAA system observed by an LAA node), and the other system (e.g., state of LAA system observed by a WLAN node), respectively. Observed by an LAA node, the probabilities of LAA channel idle, successful transmission, and failed transmission states are, respectively, given by:

$$\begin{aligned} \hat{P}_{i,L} &= (1 - \tau_L)^{n_L - 1}, \\ \hat{P}_{S,L} &= \begin{cases} (n_L - 1)\tau_L(1 - \tau_L)^{n_L - 2}, & \text{when } n_L \geq 2; \\ 0, & \text{when } n_L \leq 1, \end{cases} \\ \hat{P}_{F,L} &= 1 - \hat{P}_{i,L} - \hat{P}_{S,L}. \end{aligned}$$

However, observed by a WLAN node, the probabilities of these LAA states are given by

$$\begin{aligned} P_{i,L} &= (1 - \tau_L)^{n_L}, \\ P_{S,L} &= n_L \tau_L (1 - \tau_L)^{n_L - 1}, \\ P_{F,L} &= 1 - P_{i,L} - P_{S,L}. \end{aligned}$$

Similarly, observed by a WLAN node, probabilities of WLAN channel idle, successful transmission, and failed transmission states are, respectively, given by $\hat{P}_{i,W} = (1 - \tau_W)^{n_W - 1}$, $\hat{P}_{S,W} = \begin{cases} (n_W - 1)\tau_W(1 - \tau_W)^{n_W - 2}, & \text{when } n_W \geq 2; \\ 0, & \text{when } n_W \leq 1, \end{cases}$ and $\hat{P}_{F,W} = 1 - \hat{P}_{i,W} - \hat{P}_{S,W}$. Furthermore, observed by an LAA node, the corresponding WLAN states are $P_{i,W} = (1 - \tau_W)^{n_W}$, $P_{S,W} = n_W \tau_W (1 - \tau_W)^{n_W - 1}$, and $P_{F,W} = 1 - P_{i,W} - P_{S,W}$. Referring to Fig. 15: in an LAA CR there are 6 mutually-exclusive events, and their probability paths and durations are listed below:

- 1) All LAA and WLAN links are idle (with probability $\hat{P}_{i,L}P_{i,W}$ and duration δ_L),
- 2) successful transmission of an LAA link (with probability $\hat{P}_{S,L}P_{i,W}$ and duration $T_{S,L}$),
- 3) collision of LAA links while WLAN is idle (with probability $\hat{P}_{F,L}P_{i,W}$ and duration $T_{F,L}$),
- 4) successful transmission of a WLAN link (with probability $P_{S,W}\hat{P}_{i,L}$ and duration $T_{S,W}$),
- 5) collision of WLAN links while LAA is idle (with probability $P_{F,W}\hat{P}_{i,L}$ and duration $T_{F,W}$),
- 6) LAA-WLAN inter-system collision of transmissions (with probability $(1 - P_{i,W})(1 - \hat{P}_{i,L})$ and duration $T_{F,M}$), where $T_{F,M} = \max(T_{F,L}, T_{F,W})$.

We can verify that the probability mass function (PMF) shown in Fig. 15 sums up to unity and is valid, as shown by

$$\begin{aligned} \hat{P}_{i,L}P_{i,W} &+ \hat{P}_{S,L}P_{i,W} + \hat{P}_{F,L}P_{i,W} + P_{S,W}\hat{P}_{i,L} \\ &+ P_{F,W}\hat{P}_{i,L} + (1 - \hat{P}_{i,L})(1 - P_{i,W}) = 1. \end{aligned}$$

When $N_s = 1$, all LAA and WLAN links have a JCR opportunity at the end of each idle slot. Defining $T_{L,JCR}$ (and $T_{W,JCR}$) as the duration per CR with JCR at each LAA (and

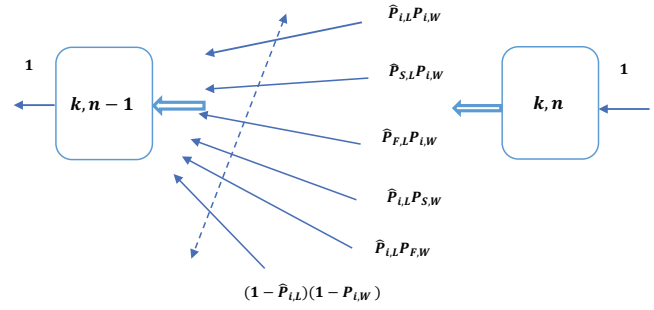


Fig. 15: Illustration of Markov model for the LAA CR when $N_s = 1$.

WLAN) link, respectively, we have:

$$\begin{aligned} T_{L,0} &= T_{L,JCR} \\ &= \hat{P}_{i,L}P_{i,W}\delta_W + (\hat{P}_{S,L}T_{S,L} + \hat{P}_{F,L}T_{F,L})P_{i,W} \\ &\quad + (P_{S,W}T_{S,W} + P_{F,W}T_{F,W})\hat{P}_{i,L} \\ &\quad + (1 - P_{i,W})(1 - \hat{P}_{i,L})T_{F,M}, \end{aligned} \quad (35)$$

$$\begin{aligned} T_{W,0} &= T_{W,JCR} \\ &= P_{i,L}\hat{P}_{i,W}\delta_W + (P_{S,L}T_{S,L} + P_{F,L}T_{F,L})\hat{P}_{i,W} \\ &\quad + (\hat{P}_{S,W}T_{S,W} + \hat{P}_{F,W}T_{F,W})P_{i,L} \\ &\quad + (1 - \hat{P}_{i,W})(1 - P_{i,L})T_{F,M}. \end{aligned} \quad (36)$$

APPENDIX C

COMPARISON WITH A RECENT METHOD ON THE COMPUTATION OF $T_{W,0}$ (WHEN $N_s = 1$)

The techniques developed in this paper explicitly compute the backoff CR time based on a novel probability path method. Below, we simplify our method to the case of a single WLAN system, and compare it with a recent WLAN analysis method [22] on the computation of $T_{W,0}$. For this special case (36) is simplified to

$$T_{W,0} = \hat{P}_{i,W}\delta_W + \hat{P}_{S,W}T_{S,W} + \hat{P}_{F,W}T_{F,W}. \quad (37)$$

We can easily verify that $\hat{P}_{i,W} + \hat{P}_{S,W} + \hat{P}_{F,W} = 1$. Based on Appendix B in an online material of [22], the hold time per WLAN CR is given by (6) of [22], which involves an approximation that $P_{i,W} = (1 - \tau_W)^{n_W - 1} \approx \exp(-n_W \tau_W)$, valid when $n_W \gg 1$. Here, we try to re-derive $T_{W,0}$ using the approach in [22] but with a more strict procedure shown next (such as without using the large- n_W assumption), and compare it with our special-case result in (37).

In [22], the CR probability at any slot t is given by α_t , and the feedback probability is $1 - \alpha_t$, where t represents a time index normalized by δ_W . We define the normalized hold time per CR as $\bar{T}_{W,0} = T_{W,0}/\delta_W$, which is derived as $\bar{T}_{W,0} = 1/\alpha_t$, where $\alpha_t = P\{\text{idle at } t\}$ is the probability that the considered node senses the channel to be idle at time t . Let ω_t , τ_T , and τ_F in [22] be replaced by τ_W , $\bar{T}_s = T_{S,W}/\delta_W$, and $\bar{T}_F = T_{F,W}/\delta_W$ respectively. It is shown in [22] that

$$\begin{aligned} \alpha_{t+1} &= P\{\text{idle at } t+1 \mid \text{idle at } t\}P\{\text{idle at } t\} \\ &\quad + P\{\text{idle at } t+1 \mid \text{success at } t\}P\{\text{success at } t\} \\ &\quad + P\{\text{idle at } t+1 \mid \text{collision at } t\}P\{\text{collision at } t\}, \end{aligned}$$

where

$$\begin{aligned}
P\{\text{idle at } t+1 \mid \text{success at } t\} &= 1/\bar{T}_S, \\
P\{\text{idle at } t+1 \mid \text{collision at } t\} &= 1/\bar{T}_F, \\
P\{\text{idle at } t+1 \mid \text{idle at } t\} &= P_{t,W} = (1 - \tau_W)^{n_W-1}, \\
P\{\text{success at } t\} &= \bar{T}_S(n_W - 1)\tau_W \\
&\quad \cdot (1 - \tau_W)^{n_W-2}, \\
P\{\text{idle at } t\} &= \alpha_t,
\end{aligned}$$

and

$$P\{\text{collision at } t\} = 1 - P\{\text{idle at } t\} - P\{\text{success at } t\}.$$

In a stationary state (as t becomes large), $\alpha_{t+1} = \alpha_t = \alpha$ holds. We have

$$\begin{aligned}
\alpha &= \alpha(1 - \tau_W)^{n_W-1} + \alpha(n_W - 1)\tau_W(1 - \tau_W)^{n_W-2} \\
&\quad + \frac{1}{\bar{T}_F}[1 - \alpha - \bar{T}_S(n_W - 1)\tau_W(1 - \tau_W)^{n_W-2}\alpha].
\end{aligned}$$

After some manipulations, we obtain

$$\bar{T}_{W,0} = 1/\alpha = 1 + \hat{P}_{S,W}\bar{T}_S + \hat{P}_{F,W}\bar{T}_F,$$

which leads to

$$T_{W,0} = \delta_W + \hat{P}_{S,W}T_{S,W} + \hat{P}_{F,W}T_{F,W}. \quad (38)$$

Since typically either $T_{S,W} \gg \delta_W$ or $T_{F,W} \gg \delta_W$ holds, or both hold, the CR time in (38) is very close to our strict result given in (37), for $N_s = 1$, though they are based on different modelling methods. In comparison, our method for deriving (37) and (36) is more concise and involves no feedback paths for $N_s = 1$. Thus, our method of probability paths is both convenient and precise, and is used as a preliminary building block in our super-counter based performance analysis for both original and ASJ-LBT schemes (when $N_s > 1$).

APPENDIX D

DERIVATION OF CR DURATIONS $T_{L,0}$ AND $T_{W,0}$ OF THE ORIGINAL-LBT (WHEN $N_s > 1$)

Please refer to the lower portion of Fig. 5. We combine the $N_s - 1$ feedback paths as one path with probability P_B , and this involves a minor approximation. Note that $P_F + P_B = 1$. If we assume that the reduction of the first $N_s - 1$ sub-counters are independent and homogeneous, we obtain $P_F \simeq P_{i,W}^{N_s-1} = (1 - \tau_W)^{(N_s-1)n_W}$, as shown by the index $(n, 0)$ in Table II. However, the assumption of homogeneous sub-counter transitions may involve a major approximation when $\tau_W \ll 1$ does not hold. We relax this assumption and develop a more accurate result next. The P_F is equal to the probability that none of the n_W WLAN nodes transmits during the first $(N_s - 1)$ sub-counters in super-counter n . The probability that a WLAN node does not transmit in this duration is given by $(1 - (N_s - 1)\tau_W)$, and the n_W WLAN nodes have independent backoff processes. Tight approximations of P_F and P_B are obtained as

$$P_F \simeq (1 - (N_s - 1)\tau_W)^{n_W}, \quad (39)$$

$$P_B = 1 - P_F \simeq 1 - (1 - (N_s - 1)\tau_W)^{n_W}. \quad (40)$$

We derive the LAA counter hold time per CR as

$$\begin{aligned}
T_{L,0} &\simeq P_F \{T_F + (1 - P_F)(T_F + T_B) + \dots \\
&\quad + (1 - P_F)^k(T_F + kT_B) + \dots\} \\
&= P_F T_F [1 + (1 - P_F) + \dots + (1 - P_F)^k + \dots] \\
&\quad + P_F [(1 - P_F)T_B + \dots + (1 - P_F)^k kT_B + \dots] \\
&= T_F + T_B(1 - P_F)/P_F. \quad (41)
\end{aligned}$$

In the first two lines of (41), factors $(1 - P_F)$ and $(1 - P_F)^k$ refer to one-time feedback and k -time feedback paths, respectively. When $0 < P_F \leq 1$, the following equality holds

$$[(1 - P_F)T_B + \dots + (1 - P_F)^k kT_B + \dots] = T_B(1 - P_F)/P_F^2.$$

In the case of WCR (with probability $P_W(\text{WCR})$), each WLAN node has average counter hold time

$$T_{W,\text{WCR}} = \hat{P}_{i,W}\delta_W + \hat{P}_{S,W}T_{S,W} + \hat{P}_{F,W}T_{F,W}.$$

In the other case of JCR with probability $P_W(\text{JCR})$, the counter hold time $T_{W,\text{JCR}}$ has the same form as (36). Thus, the average counter hold time for a WLAN node is

$$T_{W,0} \simeq P_W(\text{WCR})T_{W,\text{WCR}} + P_W(\text{JCR})T_{W,\text{JCR}}. \quad (42)$$

ACKNOWLEDGMENT

The authors thank the Editor and reviewers for some technical comments which helped improve the quality of this paper. They also thank Duncan McGillivray, Eric Anderson, Ryan Jacobs, and Michael Janezic for some helpful feedback during the preparation of this paper.

REFERENCES

- [1] R. Zhang, M. Wang, L. X. Cai, Z. Zheng, and X. Shen, "LTE-unlicensed: the future of spectrum aggregation for cellular networks," *IEEE Wireless Commun.*, vol. 22, no. 3, pp. 150–159, Jun. 2015.
- [2] F. M. Abinader, et al. "Enabling the coexistence of LTE and Wi-Fi in unlicensed bands," *IEEE Commun. Mag.*, vol. 52, no. 11, pp. 54–61, Nov. 2014.
- [3] A. Mukherjee et al., "Licensed-assisted access LTE: coexistence with IEEE 802.11 and the evolution toward 5G," *IEEE Commun. Mag.*, vol. 54, no. 6, pp. 50–57, Jun. 2016.
- [4] 3GPP TSG RAN, "Study On Licensed-Assisted Access To Unlicensed Spectrum", 3GPP TR 36.889 V13.0.0, Jun. 2015.
- [5] Ericsson, "Discussion on LBT protocols," 3GPP Tech. Rep. R1-151996, Apr. 2015.
- [6] B. Chen, J. Chen, Y. Gao, and J. Zhang, "Coexistence of LTE-LAA and Wi-Fi on 5 GHz with corresponding deployment scenarios: A survey," *IEEE Commun. Surveys Tuts.*, vol. 19, no. 1, pp. 7–32, 1st Quart., 2017.
- [7] ETSI EN 301 893 V1.8.1 (2015-03), "Broadband Radio Access Networks (BRAN); 5 GHz high performance RLAN; Harmonized EN covering the essential requirements of article 3.2 of the R&TTE Directive", March 2015.
- [8] ETSI EN 301 893 V2.1.1 (2017-05), "5 GHz RLAN; Harmonised Standard covering the essential requirements of article 3.2 of Directive 2014/53/EU," May 2017.
- [9] 3GPP TS RAN, "E-UTRA Physical layer procedures (Release 14)", 3GPP TS 36.213 V14.4.0, Sept. 2017.
- [10] IEEE LAN/MAN Standards Committee, IEEE Std 802.11-2012, Part 11: Wireless LAN Medium Access Control (MAC) and Physical Layer (PHY) Specifications, Feb. 2012.
- [11] V. Valls, A. Garcia-Saavedra, X. Costa and D. J. Leith, "Maximizing LTE capacity in unlicensed bands (LTE-U/LAA) while fairly coexisting with 802.11 WLANs," in *IEEE Commun. Lett.*, vol. 20, no. 6, pp. 1219–1222, Jun. 2016.
- [12] R. Yin, G. Yu, A. Maaref, and G. Li, "A framework for co-channel interference and collision probability tradeoff in LTE licensed-assisted access networks," *IEEE Trans. Wireless Commun.*, vol. 15, no. 9, pp. 6078–6090, Sept. 2016.

- [13] S. Han, Y. C. Liang, Q. Chen and B. H. Soong, "Licensed-assisted access for LTE in unlicensed spectrum: A MAC protocol design," *IEEE J. Sel. Areas Commun.*, vol. 34, no. 10, pp. 2550–2561, Oct. 2016.
- [14] G. Bianchi, "Performance analysis of the IEEE 802.11 distributed coordination function," *IEEE J. Sel. Areas Commun.*, vol. 18, no. 3, pp. 535–547, Mar. 2000.
- [15] I. Tinnirello, G. Bianchi, and X. Yang, "Refinements on IEEE 802.11 distributed coordination function modeling approaches," *IEEE Trans. Veh. Technol.*, vol.59, no.3, pp.1055–1067, Mar. 2010.
- [16] C. Chen, R. Ratasuk, and A. Ghosh, "Downlink performance analysis of LTE and WiFi coexistence in unlicensed bands with a simple listen-before-talk scheme," *Proc. IEEE VTC*, pp. 1–5, May 2015.
- [17] Y. Song, K. W. Sung, and Y. Han, "Coexistence of Wi-Fi and cellular with listen-before-talk in unlicensed spectrum," *IEEE Commun. Lett.*, vol. 20, no. 1, pp. 161–164, Jan. 2016.
- [18] Y. Ma and D. G. Kuester, "MAC-layer coexistence analysis of LTE and WLAN systems via listen-before-talk," in *Proc. 14th IEEE Annual Consumer Communications & Networking Conference (CCNC)*, Las Vegas, NV, 2017, pp. 534–541.
- [19] Y. Ma, D. G. Kuester, J. Coder, and W. F. Young, "Coexistence analysis of LTE and WLAN systems with heterogenous backoff slot durations," in *Proc. IEEE Int. Conf. Commun (ICC)*, Paris, 2017, pp. 1–7.
- [20] Y. Ma, W. Young, E. Anderson, and J. Coder, "Probability of coexistence of LTE-LAA and WLAN systems based on delay constraints", in *Proc. 27th ICCCN*, July 30 -August 2, 2018, Hangzhou, China, pp. 1-9.
- [21] Y. Ma, R. Jacobs, D. G. Kuester, J. Coder, and W. F. Young, "SDR-Based experiments for LTE-LAA based coexistence systems with improved design," in *Proc. IEEE GlobeCom*, Singapore, Dec. 2017.
- [22] L. Dai and X. Sun, "A unified analysis of IEEE 802.11 DCF networks: stability, throughput, and delay," *IEEE Trans. Mobile Comput.*, vol.12, no.8, pp.1558–1572, Aug. 2013.
- [23] Y. Gao, X. Sun and L. Dai, "IEEE 802.11e Std EDCA networks: modeling, differentiation and optimization," *IEEE Trans. Wireless Commun.*, vol. 13, no. 7, pp. 3863–3879, July 2014.
- [24] Y. Gao and L. Dai, "Optimal downlink/uplink throughput allocation for IEEE 802.11 DCF networks," *IEEE Wireless Commun. Lett.*, vol. 2, no. 6, pp. 627–630, Dec. 2013.
- [25] W. Zhang, M. A. Suresh, R. Stoleru and H. Chenji, "On modeling the coexistence of 802.11 and 802.15.4 networks for performance tuning," *IEEE Trans. Wireless Commun.*, vol. 13, no. 10, pp. 5855–5866, Oct. 2014.



Yao Ma (S'98-M'01-SM'08) received the B.Eng. degree from Anhui University, in 1993, the M.Sc. degree from the University of Science and Technology of China (USTC), in 1996, and the Ph.D. degree in electrical engineering from the National University of Singapore, in 2000. From 2002 to 2009, he was an Assistant Professor at the ECE department, Iowa State University, Ames IA, USA. From 2009 to 2011, he was with the EE department, Wright State University. From 2011 to 2014, he was with the Air Force Research Laboratory, Sensors

Directorate. He was later with the Infoscitex Inc. Dayton, OH, USA. Since July 2015, he has been with National Institute of Standards and Technology, Boulder CO, USA.

His research interests lie in wireless communication, networking, and signal processing. His recent research topics include spectrum sharing, wireless coexistence and uncertainty evaluation, radio resource allocation, hardware programming and experiments, and machine learning. He has been an associate editor for the IEEE Transactions on Vehicular Technology since August 2004. He was a former editor for the IEEE Transactions on Wireless Communications.



Daniel G. Kuester (S'11-M'12-SM'16) received B.S. and B.M. degrees in E.E. and music performance (2007), then M.S.E.E. (2010) and Ph.D. degrees (2012) with advisor Zoya Popovi, from the University of Colorado, Boulder. He is with the Communications Technology Laboratory at the National Institute of Standards and Technology in Boulder, CO, USA. His professional interests focus on connecting robust physical layer metrology to user-visible wireless and spectrum sharing performance. His work has been awarded the U.S. Department of Commerce Gold Medal (2017), the "Most Innovative Use of RFID" by RFID Journal (2015), and Best Paper Award by the IEEE Conf. on Wireless Power Transfer (2013).



Jason Coder received his B.S.E.E. and M.S.E.E. degrees from the University of Colorado Denver in 2008 and 2010, respectively. As a graduate student his research focused on signal processing and electromagnetics. Mr. Coder currently works in the Shared Spectrum Metrology Group as part of the National Institute of Standards and Technology's Communications Technology Laboratory. His research focuses on developing new measurement methods for spectrum sharing, wireless coexistence, and interference. This work has produced more than

45 publications in a variety of subject areas. Mr. Coder currently serves as the Chair of the ANSI C63.27 working group.



William F. Young (M'04) received the PhD degree from the University of Colorado, Boulder in Electrical Engineering in 2006.

At Sandia National Laboratories from 1998 to 2010, Dr. William Young's contributions included the information security design and assessments of Critical Infrastructure and DoD communication systems. His research included optimizing RF propagation from ad hoc wireless arrays, RF penetration of large buildings, electromagnetic interference on wireless, space-borne telemetry, and the use of MIMO channels for perimeter intrusion detection. He was with the National Institute of Standards and Technology from 2010 to 2018, where he developed RF performance test methodologies for wireless communication devices for the National Fire Protection Association (NFPA) and the ANSI C63.27 - Standard for Evaluation of Wireless Coexistence. From 2016 to 2018, he was Group Leader of Shared Spectrum Metrology and served as the technical lead for the National Advanced Spectrum and Communication Test Network (NASCTN) project investigating LTE impacts on GPS L1 Band receivers. He joined MITRE in 2018 as a subject matter expert in test and evaluation of spectrum sharing and wireless technologies. Since 2015, Dr. Young also serves as a part-time instructor at the University of Colorado, Denver.